Finite Group Lattice Gauge Theories for Quantum Simulation

Sunny Pradhan

Contents

Introduction

chapter one

Introduction to Lattice Gauge Theories

1.1 Review of Yang-Mills theory

A Yang-Mills theory is a gauge field theory on Minkowski space $\mathbb{R}^{1,d}$, where the gauge group $U(1)$ or $SU(N)$, with matter fields, which are defined by a representation of the gauge group. For example, *Quantum Chromodynamics* (QCD) is an $SU(3)$ gauge theory with Dirac spinors in the fundamental representation. Keeping in mind the example of QCD, the Lagrangian of the theory is

$$\mathcal{L} = -\frac{1}{2g^2}\mathrm{tr}(F_{\mu\nu}F^{\mu\nu}) + \overline{\psi}(i\gamma^\mu D_\mu - m)\psi, \tag{1.1}$$

where the fermions ψ are taken in the fundamental representation of $SU(N)$ and the covariant derivative is $D_\mu = \partial_\mu - iA_\mu$. We choose the convention where the Lie algebra generators T^a are Hermitian and $[T^a, T^b] = if^{abc}T^c$, with real structure constants f^{abc}. Furthermore, the generators are such that $\mathrm{tr}(T^aT^b) = \frac{1}{2}\delta^{ab}$. The strength-field tensor $F_{\mu\nu}$ is given by

$$F_{\mu\nu} = \partial_\mu A_\nu - \partial_\nu A_\mu - i[A_\mu, A_\nu] \tag{1.2}$$

and transforms in the adjoint representation of $SU(N)$. Both the gauge field A_μ and the curvature tensor $F_{\mu\nu}$ live in the Lie algebra $\mathfrak{su}(N)$.

Under a gauge transformation given by a group-valued function $g(x) \in SU(N)$, such that $\psi \mapsto g(x)\psi(x)$, then

$$A_\mu(x) \mapsto g(x)A_\mu(x)g(x)^{-1} + ig(x)\partial_\mu g(x)^{-1}, \tag{1.3}$$

so that $D_\mu\psi(x) \mapsto g(x)D_\mu\psi(x)$, while

$$F_{\mu\nu} \mapsto g(x)F_{\mu\nu}g(x)^{-1}, \tag{1.4}$$

leaving the action invariant.

The action of the theory in $d+1$ dimensions is the given by

$$S[A, \psi, \overline{\psi}] = \int \mathrm{d}^{d+1}\mathcal{L} \tag{1.5}$$

and the path integral

$$Z = \int \mathcal{D}A\mathcal{D}\overline{\psi}\mathcal{D}\psi \, e^{iS[A,\psi,\overline{\psi}]}. \tag{1.6}$$

1.1.1 Euclidean field theory

In order to work in a Euclidean space-time, we need first to perform a *Wick rotation*, where the time coordinate x_0 is mapped a forth space coordinate x_4, through $x_0 = -ix_4$. The has the effect of changing the path-integral integrand from e^{iS}, which is oscillatory, to e^{-S}, which is positive and can be interpreted as a probability distribution of the configurations of the fields.

The Euclidean path integral is

$$Z_E = \int \mathcal{D}A\mathcal{D}\overline{\psi}\mathcal{D}\psi e^{-S}, \tag{1.7}$$

so that the Minkowski action and the Euclidean action satisfy $iS_M = -S_E$. The respective actions are given by

$$S_M = \int \mathrm{d}^{d+1}x_M \mathcal{L}_M, \qquad S_E = \int \mathrm{d}^{d+1}x_E \mathcal{L}_E. \tag{1.8}$$

The rotation $x_0 = -ix_4$ leads to $\mathcal{L}_E = -\mathcal{L}_M$.

The Wick rotation does not change the form of the gauge kinetic term, i.e.,

$$-\frac{1}{2g^2}\mathrm{tr}(F_{\mu\nu}F^{\mu\nu}). \tag{1.9}$$

The sum is a simple Euclidean sum, where there are no minus signs when raising or lowering indices and $\mu = 1, \dots, d+1$.

Considering now the fermionic part of the Yang-Mills Lagrangian, we need to perform the Wick rotation on the Dirac operator. In Minkowski space-time

$$\overline{\psi}(i\gamma^\mu_M D_\mu - m)\psi = \overline{\psi}(i\gamma^\mu_M \partial_\mu + \gamma^\mu_M A_\mu - m)\psi, \tag{1.10}$$

where γ^μ_M are the gamma matrices of the Clifford algebra, and they satisfy $\{\gamma^\mu_M, \gamma^\nu_M\} = 2\eta^{\mu\nu}$. In the Euclidean Clifford algebra instead the gamma matrices γ^μ_E satisfy $\{\gamma^\mu_E, \gamma^\nu_E\} = 2\delta^{\mu\nu}$. Given the fact that we have $\partial_0 = i\partial_4$ and $A_0 = iA_4$, in order to obtain the correct form we have to put $\gamma^0_M = \gamma^4_E$. This procedure yields

$$\overline{\psi}(i\gamma^\mu_M \partial_\mu + \gamma^\mu_M A_\mu - m)\psi = -\overline{\psi}(\gamma^\mu_E \partial_\mu + i\gamma^\mu_E A_\mu + m)\psi. \tag{1.11}$$

Since $\mathcal{L}_E = -\mathcal{L}_M$, we finally arrive at

$$\mathcal{L}_E = \frac{1}{2g^2}\mathrm{tr}(F_{\mu\nu}F^{\mu\nu}) + \overline{\psi}(\gamma^\mu D_\mu)\psi, \tag{1.12}$$

where the indices are all Euclidean and $D_\mu = \partial_\mu + iA_\mu$.

1.1.2 Hamiltonian formulation

The Hamiltonian formulation of a Yang-Mills theory can be tricky, especially the part about the gauge field. Usually, one has to procede by computing the conjugate momenta and performing a Legendre transform. The main issue here is that the gauge field component A_0, does not have a conjugate momentum:

$$\frac{\partial \mathcal{L}}{\partial \dot{A}_0} = 0. \tag{1.13}$$

Hence, the transformation is not invertible. The easiest way to remedy to the situation is to impose the gauge condition $A_0 = 0$, which is called *canonical gauge* or *temporal gauge*. With this condition, the kinetic term for the gauge fields can be written as

$$\mathcal{L} = -\frac{1}{2g^2}\mathrm{tr}(F_{\mu\nu}F^{\mu\nu}) = \frac{1}{g^2}\left(\mathrm{E}^2 - \mathrm{B}^2\right) = \frac{1}{g^2}(E_i^a E_i^a - B_i^a B_i^a), \tag{1.14}$$ {eq:YM_lagrang_temporal_ga

where E and B are, respectively, the "chromoelectric" and the "chromomagnetic" fields. In the temporal gauge $\mathrm{E} = \dot{\mathrm{A}}$, the time derivative of the spatial components A of the gauge field A_μ, while B corresponds to the spatial components of the strength-field tensor $F^{\mu\nu}$ and does not involve any time derivative. From the Legendre transformation of (1.14) we obtain the Hamiltonian density:

$$\mathcal{H} = \frac{1}{g^2}E_i^a \dot{A}_i^a - \frac{1}{2g^2}(E_i^a E_i^a - B_i^a B_i^a) = \frac{1}{2g^2}\mathrm{tr}(\mathrm{E}^2 + \mathrm{B}^2), \tag{1.15}$$

hence the Hamiltonian in d spatial dimensions is

$$H = \int \mathrm{d}^d x \frac{1}{2g^2}\mathrm{tr}(\mathrm{E}^2 + \mathrm{B}^2). \tag{1.16}$$

In the Hamiltonian formulation, the fields A and E are now operators, satisfying the commutation relations

$$\begin{aligned} \left[A_i^a(x), E_j^b(y)\right] &= ig^2\delta_{ij}\delta_{ab}\delta(x-y) \\ \left[E_i^a(x), E_j^b(y)\right] &= \left[A_i^a(x), A_j^b(y)\right] = 0. \end{aligned} \tag{1.17}$$ {eq:comm_rel_E_A_continuu

The B operator is defined from A.

In order to impose the canonical gauge $A_0 = 0$, the equation of motion for A_0 has to be satisfied. This leads [citation?]to the fact that one must have

$$D_i E_i = 0, \tag{1.18}$$

where D_i are the spatial components of the covariant derivative and E_i the spatial components of the chromoelectric field. Unfortunately, the equation

above is inconsistent with the commutation relation (1.17) and so it cannot be implemented as an operator equation. The easiest solution is to impose it on states that are considered *physical*:

$$D_i E_i \left|\psi_{\text{phys}}\right\rangle = 0, \tag{1.19}$$

for each component of $D_i E_i$. The constraints select a subspace of the overall Hilbert space, which will be labeled as the *physical Hilbert space*. The condition above for a $U(1)$ theory reduces to the well known *Gauss law* $\nabla \cdot \mathrm{E} = 0$.

1.1.3 The Sign Problem

Even though interesting phases have been predicted for QCD in the $\mu - T$ plane[citation?], such as quark-gluon plasma[citation?]o superconductivity[citation?], detailed quantitative analysis has been limited to the $\mu = 0$ region only. This is due mainly to the difficulty of studying QCD in the low energy regime, where the perturbative approach fails[citation?]. Moreover, even *lattice gauge theories*, a non-perturbative approach to Yang-Mills theory (and gauge theories in general), is not applicable for $\mu \neq 0$ due to the *sign problem*.

In the Hamiltonian formulation, the chemical potential in the same manner as statistical mechanics. If $\hat{H}$ is the Hamiltonian operator and $\hat{N}$ a number operator, then one can simply replace $\hat{H}$ with $\hat{H} - \mu\hat{N}$. In the case of a Yang-Mills theory, the number operator corresponds to fermion number, i.e., $\hat{N} = \psi^\dagger\psi$.

In the path integral formalism, fermions are Grassmann variables, which we can integrate over:

$$\int \mathcal{D}\psi\mathcal{D}\overline{\psi}\exp(-\int d^{d+1}\overline{\psi}K\psi) = \det K, \tag{1.20}$$

where K is the kinetic operator for the fermions. If the fermions are coupled to gauge field, as one would expect from a Yang-Mills theory, then K has some complicated dependence on the fields A_μ. If one includes the chemical potential term $\mu\overline{\psi}^\dagger\psi$ in the Lagrangian, then the fermion determinant $\det K$ turns out to be complex[citation?], with a non-trivial phase factor.

As a result, the integrand of the path-integral is no longer positive, and it canot be interpreted as a probability distribution. This is the infamous *sign problem* and poses severe limitation to Monte Carlo simulations in the finite μ region.

1.2 Wilson approach to gauge theories

Starting from the path integral formulation, the first step in the formulation of a *lattice field theory* (LFT) is the discretization of space-time, where a discrete $d+1$-dimensional lattice substitutes the continuum space-time. The simplest choice in this regard is a hypercubic lattice with lattice spacing a, but in theory an LFT can be defined on any type of lattice. An immediate advantage of using a lattice instead of a continuum is the natural ultraviolet cutoff given by the inverse of the lattice spacing.

Formally a lattice Λ is defined as

$$\Gamma = \left\{ x \in \mathbb{R}^4 : x = \sum_{\mu=1}^{d+1} a n_\mu \hat{\mu} \quad n_\mu \in \mathbb{Z} \right\}, \tag{1.21}$$

where $\mu = 1, \dots, d+1$ and $\hat{\mu}$ is the unit vector in the direction μ. The edges will be labeled by a pair $(x, \hat{\mu})$, meaning that we are referring to the edge in the $\hat{\mu}$ direction from the vertex x. It is important to fix an orientation for each direction in the lattice. The most natural choice is to choose $+\hat{\mu}$ for each $\hat{\mu}$. So, even though $(x, \hat{\mu})$ and $(x + \hat{\mu}, -\hat{\mu})$ refers to the same link, the former is traversed in the positive direction while the latter in the negative direction.

In an LFT, both the vertices and edges (also called links) host degrees of freedom (d.o.f). In particular, the matter fields lives on the vertices while the gauge fields live on the links between vertices. However, the definition of these d.o.f. will need some care, because we have two main requirements, especially if we are interested in Yang-Mills theory:

- The lattice action should reduce to the continuum action in the continuum limit, i.e., $a \to 0$;
- The lattice action should respect the gauge symmetry.

Lorentz invariance is naturally broken on a lattice but we expect to recover it in the continuum limit.

1.2.1 Gauge fields on a lattice

[spiegazione perché usiamo il gruppo di Lie e non l'algebra di Lie] Considering a general group G, we associate an element $U_\mu(x) \in G$ to each link (x, μ). If one traverse the link in the opposite direction, one should obtain the inverse element U^{-1}. In the case of $SU(N)$, we take $U_\mu(x)$ to be the matrices in the fundamental representation. We can obtain a vector potential in the continuum limit by writing

$$U_\mu(x) = e^{iaA_\mu(x)}, \tag{1.22}$$

where a is the lattice spacing.

It is necessary to discuss about gauge invariance before moving to the dynamics of these gauge fields. A gauge transformation is described by a group-valued function $g(x)$ (in the appropriate representation), which acts on the vertices x. The variable $U_\mu(x)$ sits in the middle of the site x and $x+\hat{\mu}$, then it is reasonable to think its transformation is

$$U_\mu(x) \mapsto g(x)U_\mu(x)g(x+a\hat{\mu})^\dagger. \tag{1.23}$$ {eq:gauge_transf_field_lattice

In order to introduce a dynamics for the gauge fields $U_\mu(x)$, we need to define their action which need two satisfy two requirements: it has to be gauge-invariant and reduce to the pure gauge Yang-Mills action in the continuum limit. From (1.23), we can immediately deduce that taking the product of $U_\mu(x)$ along a closed curve will yield a gauge-invariant quantity. The simplest close curve we can consider is a *plaquette*, i.e., the smallest square face. Hence, on a plaquette $\square$ we introduce $W_\square$ to put in the action, defined as

$$W_\square = U_\mu(x)U_\nu(x+a\hat{\mu})U_\mu(x+a\hat{\nu})^\dagger U_\nu(x)^\dagger. \tag{1.24}$$ {eq:single_plaquette_Wilson_

Notice that we do not have any sum in the indices μ and ν because they are not Lorentz indices. The quantity in (1.24) is called a single plaquette *Wilson loop*.

We can only have scalar quantities in the action, so we need to take the trace of $W_\square$. Then, our lattice action will be defined as the sum over the plaquettes of $\mathrm{tr}W_\square$ (and its Hermitian conjugate):

$$\mathcal{S} = -\frac{1}{g^2}\sum_\square \left(\mathrm{tr}W_\square + \mathrm{tr}W_\square^\dagger\right). \tag{1.25}$$ {eq:wilson_action}

This is known as the *Wilson action* [citation?]. The quantity $\mathrm{tr}W_\square$ behaves as expected in the continuum limit, where we have to work with the strength field $F^{\mu\nu}$:

$$\mathrm{tr}W_\square \approx N - \frac{a^4}{2}\mathrm{tr}F_{\mu\nu}F^{\mu\nu} + \mathcal{O}(a^6), \tag{1.26}$$

The lattice action is not unique. The Wilson action in (1.25) is the simplest choice that one can make that satisfy our requirement. Some other modification, for example, can include other types of closed loops and these modification can have their place. However, they will not be considered here.

Obviously, in a path-integral formulation of lattice gauge theories we need to define the path integral, which is immediate. The partition function is given by

$$Z = \int \prod_{(x,\hat{\mu})} \mathrm{d}U_\mu(x) e^{-\mathcal{S}}, \tag{1.27}$$

where the integration measure $\mathrm{d}U_\mu(x)$ is understood to be the Haar measure. In case of a compact group, like $SU(N)$, it is well defined and yields a finite value. Now that the path integral measure has been defined, the average of an observable $\mathcal{O}$ can be computed as

$$\langle \mathcal{O} \rangle = \frac{1}{Z} \int \prod_{(x,\hat{\mu})} \mathrm{d}U_\mu(x) \mathcal{O} e^{-\mathcal{S}} \tag{1.28}$$

1.2.2 Order parameters and gauge invariance

The Wilson formulation of lattice gauge theories can resemble spin models studied in statistical mechanics. The link variables $U_\mu(x)$ can be thought as some sort of generalization of the spin degrees of freedom. They are distributed in a crystal-like structure and interact with their nearest neighbours, in this case through a four-body interaction (the plaquette action), instead of two-body interaction (like the Ising model). If one wants to pursue this analogy, then it is reasonable to look at order parameters that behaves like the spontaneous magnetization, where a non-vanishing expectation value signals a phase transition. The analogue of such an order parameter in lattice gauge theory would be something like

$$\langle U_\mu(x) \rangle \neq 0, \tag{1.29}$$ {eq:non_zero_link_var_expt_

rut it has been shown[citation?][teorema di Elitzur] that this is impossible in Wilson theory.

In standard spin models, a non-zero magnetization represents a spontaneous breaking of the global symmetry of the system. Consider the simplest case of the classical Ising model, where the degrees of freedom are binary variables $\sigma = \pm 1$. Without an external field, the energy is given by the interaction of nearest neighbouring spins, i.e., $\sigma_i \sigma_j$. This system has an obvious global $\mathbb{Z}_2$ symmetry, that corresponds to the inversion $\sigma_i \mapsto -\sigma_i$ off all the spins. A ferromagnetic phase is, by definition, signaled by $\langle \sigma \rangle \neq 0$, which necessarily breaks the global $\mathbb{Z}_2$ symmetry of the model. Once a direction is selected by $\langle \sigma \rangle \neq 0$, it remains stable under thermal fluctuations because they cannot coherently shift of the magnetization of an infinite (or rather large) number of spins.

In a lattice gauge theory, an expectation value like (1.29) would *breaks* gauge invariance, which is a *local symmetry*, not a global one. As explained previously, gauge invariance means that the action is unchanged under local arbitrary "rotations" of the link variables $U_\mu(x)$, see (1.23). Hence, thermal fluctuations will induce such rotations and in the long rung it will average on

all the possible gauges. This leads to

$$\langle U_\mu \rangle = \int \mathrm{d}U_\mu U_\mu = 0 \tag{1.30}$$

if U_μ contains only non-trivial irreducible representations of the group. This means that "magnetization" is always vanishing in a lattice gauge theory and gauge invariance cannot be spontaneously broken, which is the contents of the Elitzur theorem[citation?].

The conclusion of this brief discussion may seem rather grim, as magnetization in spin models is the most convenient and used order parameter. But this does not mean that there are no other order parameters in a lattice gauge theory. We have just showed that the problem when considering something like $\langle U_\mu \rangle$ is gauge invariance. So, the most reasonable step forward is to consider *gauge-invariant quantities*. We have already seen that tracing over a product of U_μ variables along a closed curve is a gauge-invariant quantity, called *Wilson loop*.

In so far, we have considered only single plaquette loops but nothing restraints us from considering arbitrary large loops, indeed it serves as a *confinement test* for pure gauge theories. It has been shown [citation?]that confinement is equivalent to the *area law* behaviour of Wilson loops, i.e.,

$$\langle W(\mathcal{C}) \rangle \sim \exp(-\sigma A(\mathcal{C})), \tag{1.31}$$ {eq:wilson_area_law}

where $A(\mathcal{C})$ is the minimal area inside the closed path $\mathcal{C}$ and σ the *string tension* (the coefficient of the linear potential between two quarks). On the other hand, in the absence of confinement one finds instead the *perimeter law*

$$\langle W(\mathcal{C}) \rangle \sim \exp(-kP(\mathcal{C})), \tag{1.32}$$ {eq:wilson_perimeter_law}

where $P(\mathcal{C})$ is the perimeter of the curve $\mathcal{C}$ and k just some constant.

The reason behind this behaviour can be seen with a simple qualitative picture. A closed timelike Wilson loop basically represents a process in which a quark-antiquark pair is produced, moved along the sides of the loop and annihilated. If we are confining phase we can then expect a liner potential between the quark and antiquark. We can imagine a flux tube *binding* the two charges, which swoops the whole inside the loop. Then, it is easy to image that the energy of this whole process will necessarily depend on the area of the loop. On the other hand, if we are in a deconfined phase then there is no potential binding the two quarks. In this case the energy of the whole process depends only on the self-energy of quarks, which move along the sides of the loop. Therefore, the leading energy contribution of this process depends on the perimeter, instead of the area. Obviously, this picture is no longer valid

when dynamical matter is involved. In a confining phase, pair production is always preferred when separating two quarks at large distances. [inserire immagine]

From (1.31) and (1.32), we can deduce that the string tension σ can be used as an order parameter. It is non-zero for a confining phase, while it vanishes for a deconfined phase. But it is *non-local* in nature, as it involves the asymptotic behaviour of potential, and therefore of the correlation functions of the theory.

1.2.3 Fermions on a lattice

Defining fermions is not an easy task due to the known *doubling problem*. In simple terms, when introducing fermions on a lattice, instead of a continuous space, it leads to a extra spurious fermions, which are just lattice artifacts.

In order to briefly see this, consider the correlation function for a single fermionic species. If K is the kinetic matrix for the fermions, then $G = K^{-1}$ gives their correlation matrix. One finds [citation?]that the correlation function between two sites x and y has the form

$$(G)_{x,y} = \frac{1}{a^d L^d} \sum_k \tilde{G}_k e^{2\pi i k\cdot(x-y)/L}, \tag{1.33}$$ {eq:fermionic_corr_func_real}

where a is the lattice spacing, L^d the total volume and $\tilde{G}_k$ the correlation function in momentum space:

$$\tilde{G}_k^{-1} = m + \frac{i}{a}\sum_\mu \gamma_\mu \sin(2\pi k_\mu/L). \tag{1.34}$$ {eq:fermionic_corr_func_latt}

It involves a trigonometric function because the derivative term involves nearest neighbouring sites. One can then take the model to a large lattice, which justifies in substituting the discrete sums with integrals:

$$\frac{2\pi k_\mu}{La} \to q_\mu \qquad \text{and} \qquad \frac{1}{a^d L^d}\sum_k \to \int \frac{\mathrm{d}q^d}{(2\pi)^d}, \tag{1.35}$$ {eq:limit_large_lattice}

where the q_μ's are continuous momentum variables. This substitution maps (1.34) into

$$\tilde{G}_k^{-1} = m + \frac{i}{a}\sum_\mu \gamma_\mu \sin(aq_\mu). \tag{1.36}$$ {eq:fermionic_corr_func_larg}

One can naively think of taking the limit $a \to 0$ and expand $\sin(aq_\mu)$ around the zero and obtain something that look like the correct continuum limit:

$$\tilde{G}_\mu^{-1} = m + i\not{q} + \mathcal{O}(a^2). \tag{1.37}$$

But one should not be fooled by this sloppy procedure just because it appears to give the wanted result. Each component q_μ takes values in the region $[-\pi/a, +\pi/a]$, hence we have to integrate on the whole volume $[-\pi/a, +\pi/a]^d$. Looking at (1.36), it is clear that the major contributions to G in (1.33) comes from the zeros of $\tilde{G}_k^{-1}$. This, not only vanishes in the region $q_\mu \sim 0$ but also for large momentum $q_\mu \sim \pi/a$. The propagator has no suppression of momentum values near π/a. We can isolate the large momenta region by considering

$$\tilde{q}_\mu = q_\mu - \pi/a \tag{1.38}$$

for each direction in space. In this way, we de facto half the integration region,

$$\int_{-\pi/a}^{\pi/a} \mathrm{d}q_\mu \;\to\; \int_{-\pi/2a}^{\pi/2a} (\mathrm{d}q_\mu + \mathrm{d}\tilde{q}_\mu) \tag{1.39}$$

and now the limit $a \to 0$ can be taken safely, but it comes with a price to pay. For each direction in space, we have two independent regions that gives a free fermion contribution to the propagator in the continuum limit. We have effectively *doubled* the number of fermions for each direction. In a d-dimensional lattice we end up with 2^d independent fermions, even though we initially started with just one. [qualcosa a che fare con la chiralità]

There are many solutions to this fermion doubling problem[citation?], but we will focus only on one in this manuscript: *the staggered fermions*[citation?]. We have seen that these fictitious fermions come from the large momenta regions, where $q_\mu \sim \pi/a$. Brutally cutting out this large momenta regions spoils the completeness of the Fourier transform, so it is not a solution, but a smarter solution can give out the same effect. The idea is to spread the fermionic degrees of freedom over multiple lattice sites, reducing effectively the momenta space. For example, in two dimensions it would correspond to placing the *particles* on *even* sites and the *antiparticles* on *odd* sites. A site is considered even or odd when $(-1)^x = (-1)^{x_1+\cdots+x_d} = +1$ or -1.

To obtain a staggered fermion, we define a new fermionic species $\chi(x)$ such that

$$\psi(x) = \prod_\mu (\gamma^\mu)^{n_\mu} \chi(x), \tag{1.40}$$

where $x_\mu = a n_\mu$. Now, if we want to express the discredited covariant derivative, the term $\gamma^\mu \psi(x + a n_\mu)$ have two extra powers of γ^μ compared to $\overline{\psi}$. Since $(\gamma^\mu)^2 = \pm 1$, we have therefore

$$\overline{\psi}(x) \gamma^\mu \psi(x) = (-1)^{\eta_\mu(x)} \chi(x)^\dagger \chi(x + a n_\mu), \tag{1.41}$$

where $\eta_\mu(x)$ is some sign function depending on the site x. This function can be obtained from the commutation relations of the gamma matrices. In

particular, in two dimensions we have

$$\eta_1(x) = 1 \quad \text{and} \quad \eta_2(x) = (-1)^{n_1}, \tag{1.42}$$

while in four (Euclidean) dimension we have instead [Citare Tong, gauge theories]

$$\eta_1(x) = 1, \quad \eta_2(x) = (-1)^{n_1}, \quad \eta_3(x) = (-1)^{n_1+n_2}, \quad \eta_4(x) = (-1)^{n_1+n_2+n_3}. \tag{1.43}$$

A similar reasoning can be applied to the mass term $m\overline{\psi}(x)\psi(c)$, where it becomes

$$m\overline{\psi}(x)\psi(x) = (-1)^{\eta(x)}\chi(x)^\dagger\chi(x), \tag{1.44}$$

for some sign function $\eta(x)$ that can be obtained from the commutation relations of the gamma functions.

chapter two

Quantum Simulation of Lattice Gauge Theories

2.1 Quantum simulation

Simulating quantum mechanics is a very challenging task, in particular if one is interested in many-body systems. The description of the state requires a large number of parameters, for keeping track of all the quantum amplitudes, that grows exponentially with the system size. Hence, one would have an *exponential explosion* in terms of *classical* resources (i.e., computer memory). If simulating a quantum system is not a task for classical computers, then it should be a task for *quantum computers*. This kind of devices, first envisioned from Feynman[citation?], promises much more than simulating quantum mechanics. Indeed, quantum computation and quantum information theory are, still today, very active research fields.

A quantum computer can encodes the large amount of information of a quantum system in its large number of amplitudes. So, the size of a quantum computer would only be proportional to the size of the quantum system it intends to simulate, *without* an exponential explosion in *quantum* resources. In fact, a quantum computer can indeed act as a *universal quantum simulator* (Lloyd 1996[citation?]). This is basically the idea behind *digital quantum simulations*.

However, another approach is possible. One can mimic the evolution of a given quantum system by means of another *analogous* and *controllable* quantum system. Hence, we will only need a specific quantum machine for a specific class of problems. This is, instead, the idea behind *analog quantum simulations*. In this case, for a specific set of problems the full implementation of a quantum computer may not be necessary.

In general, *quantum simulation* can be (loosely) defined as simulating a quantum system by quantum mechanical means, There are three paths that can be taken in this regard:

- digital quantum simulation

- analog quantum simulation
- quantum-information inspired algorithms for classical simulation

We will discuss briefly each one of them. By *quantum simulator* we mean a *controllable* quantum system used to simulate or emulate other quantum systems. We see that only digital and analog quantum simulations employ a quantum simulator. The last option employs techniques, inspired by quantum information theory, that make it possible to truncate and approximates quantum states in order to have efficient classical simulations.

[Inserire figura schematica di un quantum simulator]

2.1.1 Digital quantum simulations

This approach employs the circuit model for quantum computation. Generally, the quantum simulator is a collection of *qubits* (i.e., two-level quantum systems). This constitutes the *quantum register*. A wave function of the simulated system using the computation basis, in other words a superposition of binary bit string. Each bit of a string refers to the state of a qubit in the registry, which can be either $|0\rangle$ or $|1\rangle$ in the computational basis. On this register, any many-qubit unitary transformation U is implemented through the application of a sequence of single- and two-qubit unitary operations, called *quantum gates*. An immediate example of relevant unitary transformation is the time-evolution operator, that solves the time-independent Schrödinger equation.

Even though it has been proven (Lloyd 1996[citation?]) that "anything" can be simulated on a quantum computer, not all unitary operations can be simulated *efficiently*. Therefore, there are *mathematically possible* Hamiltonians that cannot be efficiently simulated with a circuit-based model. Luckily, it is believed that *physically relevant* Hamiltonians can indeed be simulated efficiently. Furthermore, it should be stressed that the implemented unitary operations are often just approximations of the desired unitary operation. With greater precision comes a greater number of gates.

The typical setup for a digital simulation is made of three steps:

- *Initial-state preparation* — where the quantum register has to prepared in the state $|\psi(0)\rangle$. This step can be by itself difficult, and it is not always guaranteed that an efficient algorithm may exist.
- *Unitary evolution* — where the circuit has to reproduce or simulate the action of a unitary operator U. In case of a unitary time evolution

and local Hamiltonian this can be achieved approximately with some "trotterization" scheme.

- *Final measurement* — after obtained the wanted state $|\psi(t)\rangle = U|\psi(0)\rangle$, a *measurement* is needed in order to extract the relevant physical information. Instead of capturing the whole wave function $|\psi(t)\rangle$, with for example quantum tomography, one may proceed with the direct estimation of certain physical quantities, such as correlation functions or spectra of operators.

2.1.2 Analog quantum simulations

Analog quantum simulation (AQS) in another possible approach to quantum simulation, where a one quantum system mimics or emulate another. The Hamiltonian of the system to be simulated H_{sys} is directly mapped onto the Hamiltonian of the simulator H_{sim}. Obviously, this can be done if there is a mapping between the system and the simulator. Note that the simulator may only partly reproduce the dynamics of the system, or simulate some effective description of the system.

An important advantage of AQS is that it does not require a full quantum computer, even more the simulator does not even need to be a computer at all. Finding the mapping in an AQS might look, at first, simpler than finding the most efficient gate decomposition of a Hamiltonian, but it is not always guaranteed and there are no recipes ready for such mappings. The obvious drawback of AQS is that the quantum simulators are problem specific.

[Aggiungere altro]

2.1.3 Quantum-inspired algorithms

Classical numerical algorithms for the simulation of quantum many-body systems came out of research on quantum information theory in these later years. The most important examples of quantum-inspired algorithms are *tensor networks* methods. Tensor networks make it possible to compress the information about a many-body wave function by expressing it as a contraction of a network of tensors (as suggested by the name). For a large class of physically relevant models, the ground state is gapped and has, in a certain sense, a finite amount of entanglement. This fact is expressed by the so-called *area law*, where the entanglement between two partitions of the system grows with size of the boundary, the area between the two partitions, and not with the size of the partition itself. The main advantage of tensor networks is their ability to capture this area law.

[Aggiungere altro]

2.2 Quantum simulation for gauge theories

The problem of lattice gauge theories is arguably one of the most computationally intensive quantum many-body problem of all, due to the large numbers of degrees of freedom per site and the necessity of simulation in three spatial dimensions. We have already show a formulation of LGT in the path integral formalism. It can be used for simulations with Monte Carlo methods and indeed it already quite some results [inserire quali][citation?]. However, Monte Carlo methods suffers some problem. Simulation in Euclidean space time cannot approach several problems. For example, we already shown that the presence of fermionic matter leads to the so-called sign problem, which makes it very difficult to simulate situations with finite chemical potential. Another desirable feature it the real time evolution in Minkowski space time, which is absent when time is imaginary.

Recently, different approaches have been proposed for the quantum simulation of LGTs, from different communities, one for each possible path in quantum simulation (showed previously). For quantum-inspired classical simulation, different methods have been proposed for the simulation of LGTs using *tensor networks states*, to study the ground state, time evolution, and phase structure with both numerical and analytical models. The second type of approach relies on *analog simulation* with different kind of controllable experimental devices. The options ranges from ultracold atoms in optical lattices[citation?], trapped ions[citation?], or superconducting qubits[citation?]. The proposals have addressed LGTs of different levels of complexity, Abelian or non-Abelian, with or without dynamical matter, etc.... The last but not the least type of approach is digital quantum simulation, where the task of simulating the theory is done by a quantum computer. We will mainly focus on this last approach.

In order to be able to simulate a LGT on a quantum computer, some kind of *digitization* of the fields is necessary. By digitization, we mean the task of formulation, representing, and encoding QFT (choosing the basis) in ways useful for computational calculations. The lattice field theory, presented in Sec. 1.2, is the most conventional digitization scheme of non-perturbative field theory but it is only feasible for classical computers. It relies on resources far beyond near-term quantum computers. In conventional LGT, fermionic fields are integrated out, leaving a non-local action. A direct application of this procedure to quantum computers would require a high connectivity between qubits. Furthermore, for bosons, LGT works with bosons (i.e., the

gauge fields) which have a infinite-dimensional local Hilbert space. This is prohibited on a real quantum computer, where we have only finite quantum registers. We will show the different tactics for solving this issue later in the chapter

The starting point for a digital simulation of a LGT is its Hamiltonian formulation. This has been worked by Kogut and Susskind in their seminal paper[citation?], the starting point for any endeavour in quantum simulation of LGTs, which we will review in the following section

2.3 Kogut-Susskind Hamiltonian formulation

The classical formulation of Hamiltonian LTG is due to Kogut and Susskind, in [citation?]. It can be regarded as the Hamiltonian corresponding to the Wilson action [inserire eqref]. The former can be obtained from the latter by the transfer matrix technique[citation?], where two different lattice spacing are assigned to time and spatial dimensions and then the continuum limit for the time direction is taken. Another derivation can be done by means of Legendre transform, but in this text we will adopt a more modern approach, based on [citare Milsted, Osborne 2018].

As one can expect, the Kogut-Susskind Hamiltonian H_{KS} is made of two terms, the electric part and the magnetic part:

$$H_{\mathrm{KS}} = H_E + H_B. \tag{2.1}$$

These will be constructed separately and for a simple reason. The magnetic term involves only the spatial component of the field strength tensor, i.e., $\boldsymbol{B}^2 \sim F^{ij}F_{ij}$, while the electric term involves also the temporal components, i.e., $\boldsymbol{E}^2 \sim F^{0i}F_{0i}$. Given that in the Hamiltonian formalism time is continuous while space is discrete, the two terms cannot be treated on the same footing. This differs from the Wilson action approach, where the magnetic and electric are treated equally because it has to be Lorentz-invariant.

Another point of divergence with the path-integral approach is that now both the electric field and magnetic term are operators, not simple variables. In order to have well-defined, or defined at all, operators we have to define the appropriate Hilbert space on which these operators act.

2.3.1 Single link Hilbert space and operators

We start by considering a single link ℓ and define the gauge degrees of freedom. In the construction in Sec. 1.2.1, given a gauge group G we have associated an element $g \in G$ to the link ℓ. Hence, the configuration space for each link

ℓ is exactly G. When quantizing, the configuration space G is elevated to a Hilbert space $\mathcal{H}^G$ which is spanned by the elements $g \in G$:

$$\mathcal{H}^G \equiv \text{span}\{|g\rangle : g \in G\}, \tag{2.2}$$ {eq:single_link_Hilbert_space}

where the set $\{|g\rangle\}$ is an orthonormal basis. Therefore, an element $|\psi\rangle$ of $\mathcal{H}^G$ can be written as

$$|\psi\rangle = \int \mathrm{d}g\, \psi(g)\, |g\rangle\,, \tag{2.3}$$

where $\int \mathrm{d}g$ is a proper measure in the case of continuous groups (usually the Haar measure) or a simple sum in case of finite groups. In the former case $\mathcal{H}^G$ is equivalent to the space $L^2(G)$ of square-integrable functions of G, i.e., each element $|\psi\rangle$ can be identified with the functions $\psi(g)$. While in the latter case, the space $\mathcal{H}^G$ is equivalent to the so-called group algebra $\mathbb{C}[G]$. The total Hilbert space of the model is simply given by the tensor product

$$\mathcal{H}_{\text{tot}} = \bigotimes_{\ell} \mathcal{H}^G_\ell \tag{2.4}$$

Focusing now on the case of continuous groups like $\text{SU}(N)$, given a single link Hilbert space $\mathcal{H}^G_\ell$, the first set of operators we can define on it are the *position observables* $\hat{u}_{mn}$, via

$$\hat{u}_{mn}\, |g\rangle = U(g)_{mn}\, |g\rangle\,, \tag{2.5}$$

where $U(g)_{mn}$ is the matrix element (m,n) of $U(g)$, the image of g in the fundamental representation U of G. One can then define a matrix of operators $\hat{u}$, whose elements are precisely the operators $\hat{u}_{mn}$. Note that $\hat{u}$ is unitary as long as the chosen representation is unitary, but this not guarantee that each operator $\hat{u}_{mn}$ is unitary. Indeed, it can be shown that $(\hat{u}_{mn})^\dagger = (\hat{u}^\dagger)_{mn}$.

A second set of operators can be defined on $\mathcal{H}^G$, which makes use of the group structure of G. For each element $h \in G$, we define L_h and R_h such that for any $|g\rangle \in G$

$$L_h\, |g\rangle = |hg\rangle \quad \text{and} \quad R_h\, |g\rangle = |gh^{-1}\rangle\,, \tag{2.6}$$

which are the *left* and *right* multiplication operators, respectively. If the basis $\{|g\rangle\}$ is considered as the "position basis" then the operators L_h and R_h can be regarded as "translation operators". The left multiplications commutes with the rights one and both L_h and R_h respects the group structure of G, i.e.,

$$L_g L_h = L_{gh} \quad \text{and} \quad R_g R_h = R_{gh}, \tag{2.7}$$

indeed the maps $\hat{L} : h \mapsto L_h$ and $\hat{R} : h \mapsto R_h$ are basically *regular representations* of the group G. It can also be shown that L_h and R_h are unitary operators and satisfy

$$(L_h)^\dagger = (L_h)^{-1} = L_{h^{-1}} \quad \text{and} \quad (R_h)^\dagger = (R_h)^{-1} = R_{h^{-1}}. \tag{2.8}$$

2.3.2 Magnetic Hamiltonian

As already mentioned, it is relatively easy to obtain the magnetic term if we already know the Wilson approach but it order to make the presentation clear we repeat the step for major clarity.

Fixing the lattice orientation, on a link ℓ we define

$$\hat{u}_{mn}(\ell) = \begin{cases} \hat{u}_{mn} & \text{if } \ell \text{ traversed in the positive direction,} \\ \hat{u}_{mn}^\dagger & \text{if } \ell \text{ traversed in the negative direction.} \end{cases} \tag{2.9}$$

Then, let γ be a oriented path, which we write as $\gamma = \langle \ell_1 \ell_2 \dots \ell_q \rangle$. Next, on γ we can define the *Wilson line* W_γ whose matrix elements are

$$(W_\gamma)_{mn} = \sum_{m_1 \dots m_{q-1}} \hat{u}_{m m_1}(\ell_1) \hat{u}_{m_1 m_2}(\ell_2) \cdots \hat{u}_{m_{q-1} n}(\ell_q), \tag{2.10}$$

which can be written in a more compact way as

$$W_\gamma = \hat{u}(\ell_1)\hat{u}(\ell_2)\cdots\hat{u}(\ell_n), \tag{2.11}$$

where the matrix multiplication is implied. When considering closed path, we can take the trace of W_γ in order to have no free matrix indices:

$$\mathrm{tr} W_\gamma = \sum_m (W_\gamma)_{mm} \tag{2.12}$$

Since $\boldsymbol{B}^2 = \frac{1}{2} F_{ij} F^{ij}$, we can copy the spatial part of the Wilson formulation and consider single plaquette Wilson loops:

$$\mathrm{tr} \hat{W}_\square = \mathrm{tr}\Big(\hat{u}(\ell_1)\hat{u}(\ell_2)\hat{u}(\ell_3)^\dagger \hat{u}(\ell_4)^\dagger \Big), \tag{2.13}$$

where $\ell_1, \dots, \ell_4$ are the links around a purely spatial plaquette. Thus, the magnetic Hamiltonian is

$$H_B = -\frac{1}{g^2 a^{4-d}} \sum_\square \Big(\mathrm{tr} W_\square + \mathrm{tr} W_\square^\dagger \Big), \tag{2.14}$$

where the sum is over the plaquettes of lattice and the coupling is chosen in order to have the correct limit.

2.3.3 Electric Hamiltonian

The construction of the electric term of the Hamiltonian is less trivial, since we cannot use Wilson loops in the time direction. Recall that in the continuum theory the electric field is the infinitesimal generators of translations of the gauge fields. Hence, we have to find the infinitesimal generators corresponding

to the "translations" L_h and R_h. From these then we can build the electric Hamiltonian. In the case of Lie groups there is a recipe we can use for these generators.

So, consider the case of a compact Lie group G and its Lie algebra $\mathfrak{g}$. Given that $\hat{L} : h \mapsto L_h$ and $\hat{R} : h \mapsto R_h$ are regular representations of the Lie group G, we can easily find the regular representations of the Lie algebra. This is a linear map that maps every element $X \in \mathfrak{g}$ into an element $\hat{\ell}(X)$ such that

$$L_{e^{i\epsilon X}} = \exp\Big(i\epsilon \hat{\ell}_L(X)\Big) \quad \text{and} \quad R_{e^{i\epsilon X}} = \exp\Big(i\epsilon \hat{\ell}_R(X)\Big). \tag{2.15}$$

The maps $\hat{\ell}_L$ and $\hat{\ell}_R$ are the left and right Lie algebra representations. It does not matter which one we use, so we chose the left representation. Similar calculation can be carried out with the right one as well.

If L_h is unitary, then $\hat{\ell}(X)$ is necessarily Hermitian. Let $\{T^a\}$ be the Hermitian generators of $\mathfrak{g}$ with commutation relations

$$[T^a, T^b] = if^{abc}T^c, \tag{2.16}$$ {eq:Lie_algebra_comm_relati

where f^{abc} are the structure constants. Obviously, $X \mapsto \hat{\ell}_L(X)$ is a ordinary Lie group representation (not to be confused with regular representation). Hence, we can defined the momentum operators as the images of the generators T^a through $\hat{\ell}_L$:

$$\hat{\ell}^a_L \equiv \hat{\ell}_L(T^a), \tag{2.17}$$

and they automatically satisfy (2.16),

$$\left[\hat{\ell}^a_L, \hat{\ell}^b_L\right] = if^{abc}\hat{\ell}^c_L. \tag{2.18}$$

Alternatively, the operators $\hat{\ell}^a_L$ can also be obtained by differentiating L_h:

$$\hat{\ell}^a_L = -i\frac{\mathrm{d}}{\mathrm{d}\epsilon}L_{e^{i\epsilon T^a}}\Big|_{\epsilon=0} \tag{2.19}$$

The operators $\hat{\ell}^a_L$ will act as "conjugate variables" to the operators $\hat{u}$, with commutation relations

$$[\hat{\ell}^a_L, \hat{u}] = -T^a\hat{u}. \tag{2.20}$$

Bearing in mind that the continuum Hamiltonian contains the square of the electric field, we may then form the group Laplacian on a link ℓ as the square of the generators $\hat{\ell}^a_L$:

$$\Delta_\ell = \sum_a \left(\hat{\ell}^a_L\right)^2. \tag{2.21}$$

This is a Laplacian on the space $L^2(\mathrm{SU}(N))$, in an entirely analogous way to the Laplacian operator of ordinary quantum mechanics, which is given by the sum of squares of the infinitesimal generators of translations in each space direction. With the continuum limit in mind, then the correct form the electric Hamiltonian is

$$H_E = \frac{g^2}{2a^{d-2}} \sum_{\ell} \Delta_\ell = \sum_{\ell} \sum_{a} \left(\hat{\ell}_L^a\right)^2 \tag{2.22}$$

where the sum is taken over the links of the lattice. Therefore, the overall Kogut-Susskind Hamiltonian is given by

$$H = \frac{g^2}{2a^{d-2}} \sum_{\ell} \Delta_\ell - \frac{1}{g^2 a^{4-d}} \sum_{\square} \left(\mathrm{tr} W_{\square} + \mathrm{tr} W_{\square}^{\dagger}\right) \tag{2.23}$$

2.3.4 Gauge transformations

chapter three

Dualities in Abelian Models

3.1 Toric Code and its features

The Toric code is two-dimensional model of spin-$\frac{1}{2}$degrees of freedom (d.o.f). It can be regarded as an example of a pure $\mathbb{Z}_2$ lattice gauge theory. In particular we focus on a $L \times L$ square lattice (with periodic boundary conditions), and the d.o.f. are defined on the links the lattice. The local Hilbert space is $\mathbb{C}^2$ and as a basis we can use the computation basis (or Z-basis) $\{|0\rangle, |1\rangle\}$ for which the Pauli matrix σ^z (shortened as Z) is diagonal. The main local operators (that enters the Hamiltonian) are defined on the *stars* (the links attached to a given site) and *plaquettes* (links around a face) of the lattice:

$$A_v = \prod_{j \in \text{star}(s)} \sigma_j^z, \qquad B_p = \prod_{j \in \partial p} \sigma_j^x. \tag{3.1}$$

One can easily prove the following commutation relations of the A_ss and B_ps operators

$$[A_v, A_{v'}] = 0, \quad [B_p, B_{p'}] = 0, \quad [A_v, B_p] = 0 \tag{3.2}$$ {eq:star_plaq_op_comm}

for all v, v' and p, p'. The eigenvalues of the Pauli matrices are just $pm1$, so the same holds true for A_s and B_p. Moreover, like the Pauli matrices, also $A_s^2 = \mathbb{1}$ and $B_p^2 = \mathbb{1}$.

Now, we proceed with writing the Toric Code Hamiltonian:

$$H = -\sum_v A_v - \sum_p B_p \tag{3.3}$$ {eq:toric_code_hamiltonian}

which is *exactly solvable*. Indeed, given (3.2), one can find a ground state $|\Omega\rangle$ by simply imposing a set of constraints

$$A_v |\Omega\rangle = |\Omega\rangle, \qquad B_p |\Omega\rangle = |\Omega\rangle, \qquad \forall v, \tag{3.4}$$ {eq:ground_state_constraints

Even more, it is possible to define the set of ground states

$$\mathcal{L} = \{|\Omega\rangle : A_s |\Omega\rangle = |\Omega\rangle, \quad B_p |\Omega\rangle = |\Omega\rangle \quad \forall s, p\} \tag{3.5}$$

which contents *depends on the topology of the lattice*. For example, if the lattice has periodic boundary conditions, then there are 4 degenerate ground states $|\Omega_{u,v}\rangle$ with $u, v = \pm 1$, which can be distinguished only by non-local operators. We will see how later.

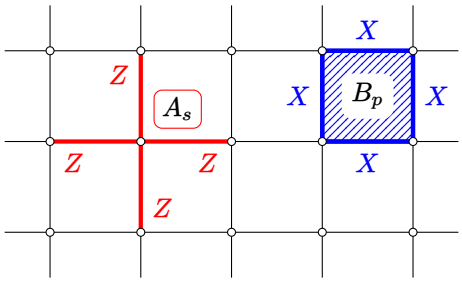

Figure 3.1: Graphical representation of the Toric Code operators A_s and B_p

3.1.1 Ground states

Consider a torus geometry for the lattice, i.e. periodic boundary conditions in both directions, of size $L \times L$. From (3.4), we have $2L^2$ constraints but these are not all independent. In fact on a torus, one can see that

$$\prod_v A_v = \mathbb{1}, \qquad \prod_p B_p = \mathbb{1} \tag{3.6}$$

which actually means that there are $2L^2 - 2$ independent conditions. The total Hilbert space has dimension 2^{2L^2}, therefore the space $\mathcal{L}$ has dimension $2^{2L^2-2L^2+2} = 4$, which means that the Toric Code has 4 degenerate ground states. These states all satisfy the same set (3.4) of equations, which means that they *cannot be distinguished by local operators*. This is typical of topological phases in two dimensions [ref].

These ground states can only be distinguished by non-local operators that have to commute with Hamiltonian in (3.3), hence with all A_v and B_p but cannot be expressed in terms of A_v and B_p. The only operators that satisfy this requirements are defined on closed paths, on the direct or dual lattice, that cannot be reduced to a single plaquette loop (on the dual lattice the plaquettes are the stars of the direct lattice). In other words, they are defined along *non-contractible loops*. The reason being that any product of σ^x or σ^z along a closed curve $\mathcal{C}$ that commutes with the Hamiltonian can be expressed as product of A_v or B_p of the stars or plaquettes enclosed by $\mathcal{C}$. Consider now, two non-contractible curves $\mathcal{C}_1$ and $\mathcal{C}_2$ along the $\hat{1}$ and $\hat{2}$ direction respectively. On these paths we can define the *string operators*

$$\overline{X}_1 = \prod_{j \in \mathcal{C}_1} \sigma_j^x, \qquad \overline{X}_2 = \prod_{j \in \mathcal{C}_2} \sigma_j^x, \tag{3.7}$$

{eq:nonlocal_X_operators}

it can be proved that they commute with all the local operators but cannot be expressed as a product of them. The same can be repeated on the dual

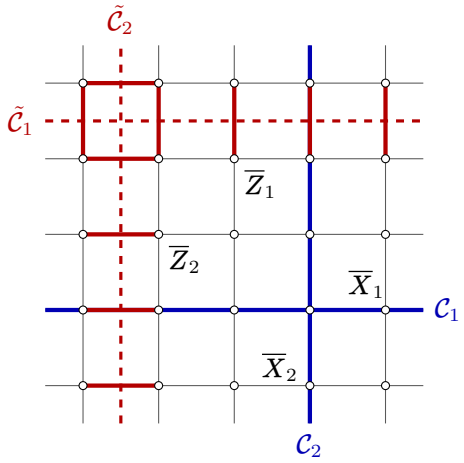

Figure 3.2: Non-contractible paths

lattice, by considering dual non-contractible paths $\tilde{\mathcal{C}}_1$ and $\tilde{\mathcal{C}}_2$ and defining

$$\overline{Z}_1 = \prod_{j \in \tilde{\mathcal{C}}_1}, \qquad \overline{Z}_2 = \prod_{j \in \tilde{\mathcal{C}}_2} \tag{3.8}$$ {eq:nonlocal_Z_operators}

Likewise, the operators in (3.8) commutes with all the vertex and plaquettes operators but they do not commute with the X-operators in (3.7).

In fact, (3.7) and (3.8) have the same (anti)commutation relations of two qubits:

$$\left\{\overline{X}_1, \overline{Z}_2\right\} = 0, \qquad \left\{\overline{X}_2, \overline{Z}_1\right\} = 0, \tag{3.9}$$

Therefore, the Toric Code (on a torus) has a protected subspace $\mathcal{L}$ (the space of the ground states) that behaves like the Hilbert space of two qubits and the operators (3.7) and (3.8) acts like unitary gates on this space.

[revisionare]

3.1.2 Particle excitations

Until now we have only discussed the ground states of the Toric Code, without touching the rest of the low energy sectors. In other words, how do we describe the excitations of this model? As we said, (3.4) are the set of constraints that defines the ground states. Therefore, everytime a given state $|\Psi\rangle$ violates these equations, we will say that it contains *particles*, which can be of different types. If $A_v |\Psi\rangle = -|\Psi\rangle$, then we will say that the vertex v contains a z-type particle. Likewise, if $B_p |\Psi\rangle = -|\Psi\rangle$, then the plaquette p contains a x-type particle.

Now the question: starting from a ground state $|\Omega\rangle$, how can we introduce some particles? The answer is *string operators*. We are not considering closed

strings, like we did in Sec. 3.1.1, but any open string. The shortest open string that we can consider is a single link. So a Z-string on a single link is just Z_j, where j is a label of a generic link. Consider now the state

$$|\Psi^Z\rangle = Z_j |\Omega\rangle , \tag{3.10}$$

This state hosts particles at the "boundaries" of the j-th link, i.e. the vertices touching j which we call v_0 and v_1. This can be proved by simply showing that $[A_v, Z_j] = 0$ for $v \neq v_0$ and $v \neq v_1$ and $\{A_{v_0}, Z_j\} = \{A_{v_1}, Z_j\} = 0$. Which immediately implies that

$$A_{v_0} |\Psi^Z\rangle = A_{v_1} |\Psi^Z\rangle = - |\Psi^Z\rangle \tag{3.11}$$

3.2 $\mathbb{Z}_N$ Model

In this section we are going to consider a class of Abelian lattice gauge theories (LGTs) on a two-dimensional lattice with a discrete symmetry $\mathbb{Z}_N$. Then we will restrict these models on a *ladder geometry*, which will be defined more precisely later.

3.2.1 Schwinger-Weyl algebra

According to Wilson's Hamiltonian approach to lattice gauge theories [28], $U(1)$ gauge fields are defined on the links of a lattice $\mathbb{L}$ either in a pair of conjugate variables, the electric field E_ℓ and either the vector potential A_ℓ, satisfying $[E_\ell, A_{\ell'}] = i\delta_{\ell,\ell'}$, or equivalently the magnetic operator, also called comparator, $U_\ell = e^{-iA_\ell}$, such that $[E_\ell, U_{\ell'}] = \delta_{\ell,\ell'} U_\ell$, all acting on an infinite dimensional Hilbert space defined on each link. This form of the canonical commutation relations represents the infinitesimal version of the relations: $e^{i\xi E} e^{-i\eta A} e^{-i\xi E} = e^{i\xi\eta} e^{-i\eta A}$, for any $\xi, \eta \in \mathbb{R}$, that define the Schwinger-Weyl group [15, 6, 22].

For a discrete group like $\mathbb{Z}_N$, the notion of infinitesimal generators loses any meaning and we are led to directly consider, for each link $\ell \in \mathbb{L}$, two unitary operators V_ℓ, U_ℓ, such that [22, 21]

$$V_\ell U_\ell V_\ell^\dagger = e^{2\pi i/N} U_\ell, \qquad U_\ell^N = \mathbb{1}_N, \qquad V_\ell^N = \mathbb{1}_N. \tag{3.12}$$ {eq:schwinger_weyl_algebra}

while on different links they commute. Thus, by representing $\mathbb{Z}_N$ with the set of the N roots of unity $e^{i2\pi k/N}$ $(k = 1, \cdots, N)$, commonly referred to as the discretized circle, we see that V plays the role of a "position operator" on the discretized circle, while U that of a "momentum operator".

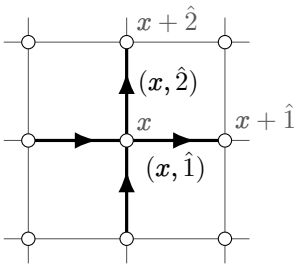

Figure 3.3: Labelling of the sites and the links in the two dimensional lattice. A site is labeled simply with $x = (x_1, x_2)$, while $\hat{1} = (1, 0)$ and $\hat{2} = (0, 1)$ stand for the unit vectors of the lattice. A link ℓ is denoted with a pair $(x, \pm\hat{\imath})$, with $\hat{\imath} = \hat{1}, \hat{2}$.

These algebraic relations admit a faithful finite-dimensional representation of dimension N [26], for any integer N, which is obtained as follows. To each link ℓ, we can associate an N-dimensional Hilbert space $\mathcal{H}_\ell$ generated by an orthonormal basis $\{|v_{k,\ell}\rangle\}$ $(k = 1, \dots, N)$, called the *electric basis*, that diagonalizes V_ℓ. With this choice, we can promptly write the actions of U_ℓ and V_ℓ:

$$\begin{aligned} U\,|v_{k,\ell}\rangle &= |v_{k+1,\ell}\rangle\,, & U\,|v_{N,\ell}\rangle &= |v_{1,\ell}\rangle \\ U^\dagger\,|v_{k,\ell}\rangle &= |v_{k-1,\ell}\rangle\,, & U^\dagger\,|v_{1,\ell}\rangle &= |v_{N,\ell}\rangle \\ V\,|v_{k,\ell}\rangle &= \omega^k\,|v_{k,\ell}\rangle\,, & V^\dagger\,|v_{k,\ell}\rangle &= \omega^{-k}\,|v_{k,\ell}\rangle\,. \end{aligned} \tag{3.13}$$

{eq:elect_basis_op_action}

where $\omega = e^{2\pi i/N}$ and $k = 0, \dots, N-1$. We choose to work in this particular basis and the various k can be interpreted as the quantized values of the electric field on the links.

On a two-dimensional square lattice of size $L \times L$, the links ℓ of the lattice can also be labeled with $(x, \pm\hat{\imath})$, where $x \in \mathbb{L}$ is a site and $\hat{\imath} = \hat{1}, \hat{2}$ the two independent unit vectors. In this way, $(x, \pm\hat{\imath})$ will refer to the link that start in x and goes in the positive (negative) direction $\hat{\imath}$ (see Fig. 3.3). This notation will be simplified when we reduce to the ladder case.

3.2.2 Gauge invariance and physical states

Gauge transformations act on vector potentials while preserving the electric field. For a $U(1)$ gauge theory, a local phase transformation is induced by a real function α_x defined on the vertices $x \in \mathbb{L}$, such that $A_\ell \to A_\ell + (\alpha_{x_2} - \alpha_{x_1})$ or equivalently $U_\ell \to e^{i(\alpha_{x_2} - \alpha_{x_1})E_\ell} U_\ell e^{-i(\alpha_{x_2} - \alpha_{x_1})E_\ell}$, where x_1, x_2 are the initial and final vertices of the (directed) link ℓ. In the case of a discrete symmetry, a gauge transformation at a site $x \in \mathbb{L}$ is a product of V's (and $V^\dagger$'s) defined on

the links which comes out (and enters) the vertex. More specifically, for a two dimensional lattice, if the link ℓ at site x is oriented in the positive direction, i.e. either $(x, +\hat{1})$ or $(x, +\hat{2})$, then V is used, otherwise $V^\dagger$. Thus, the single local gauge transformation at the site x is enforced by the operator:

$$G_x = V_{(x,\hat{1})} V_{(x,\hat{2})} V^\dagger_{(x,-\hat{1})} V^\dagger_{(x,-\hat{2})}, \tag{3.14}$$ {eq:gauss_operator}

as shown in the left part of in Fig. 3.4.

The whole operator algebra $\mathcal{A}$ of the theory is generated by the set of all U_ℓ and V_ℓ (and their Hermitian conjugates) of all the links of the lattice $\mathbb{L}$, while the *gauge-invariant subalgebra* $\mathcal{A}_{\text{gi}}$ consists of operators that commutes with all the G_x:

$$\mathcal{A}_{\text{gi}} = \{O_{\text{gi}} \in \mathcal{A} \ : \ [O_{\text{gi}}, G_x] = 0 \quad \forall x \in \mathbb{L}\}. \tag{3.15}$$

Using (3.14) and recalling (3.12), it is possible to see that the V_ℓ's commute with G_x (as expected), while the U_ℓ's do not. In spite of that, we can build gauge-invariant operators out of the comparators U_ℓ. Consider a *plaquette* $\square$ of the lattice $\mathbb{L}$ at x, by which we mean the face of the lattice with vertices $\{x, x+\hat{1}, x+\hat{1}+\hat{2}, x+\hat{2}\}$ in the counterclockwise order, as shown in the right part of Fig. 3.4. On this plaquette, the operator $U_\square$ is defined as

$$U_\square = U_{(x,\hat{1})} U_{(x+\hat{1},\hat{2})} U^\dagger_{(x+\hat{1}+\hat{2},-\hat{1})} U^\dagger_{(x+\hat{2},-\hat{2})}. \tag{3.16}$$ {eq:plaq_operator}

and one finds out that the $U_\square$'s commute with G_x, for all $x \in \mathbb{L}$, thus giving a generator of $\mathcal{A}_{\text{gi}}$.

The set $\{U_\square, V_\ell\}$ (for all plaquettes $\square$ and all links ℓ) may not be enough to generate the whole algebra $\mathcal{A}_{\text{gi}}$, in case of periodic boundary conditions. In order to prove this, consider a lattice $\mathbb{L}$, periodic in both dimensions, and denote with $\mathcal{C}_1$ and $\mathcal{C}_2$ any two *non-contractible loops* around the lattice, that extends along the $\hat{1}$ and $\hat{2}$ direction respectively. Then, define the (Wilson loop) operators $\overline{W}_1$ and $\overline{W}_2$ (pictured in blue in Fig. 3.5):

$$\overline{W}_i = \prod_{\ell \in \mathcal{C}_i} U_\ell, \qquad i = 1, 2. \tag{3.17}$$ {eq:top_wilson_loop}

A simple calculation shows that both $\overline{W}_1$ and $\overline{W}_2$ commute with all G_x, thus they are gauge-invariant, but one also finds out that none of them can be written as a product of $U_\square$ nor V_ℓ. Therefore they have to be added explicitly to the set of generators of $\mathcal{A}_{\text{gi}}$ in order to obtain the whole algebra. These operators $\overline{W}_1$ and $\overline{W}_2$ play a fundamental role in the model to define topological sectors of the theory, as we will see later.

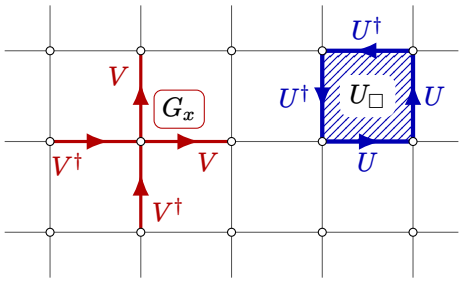

Figure 3.4: Pictorial representation of the Gauss operators G_x in (3.14) (*left*) and plaquette operator $U_\square$ in (3.16) (*right*).

The total Hilbert space $\mathcal{H}^{\text{tot}}$ is given by the $\otimes_\ell \mathcal{H}_\ell$. A state of the whole lattice $|\Psi_{\text{ph}}\rangle \in \mathcal{H}^{\text{tot}}$ is said to be *physical* if it is a *gauge-invariant state*:

$$G_x |\Psi_{\text{ph}}\rangle = |\Psi_{\text{ph}}\rangle\,, \qquad \forall x \in \mathbb{L} \tag{3.18}$$ {eq:gauss_law}

This condition can be translated into a constraint on the eigenvalues $v_{(x,\pm\hat{i})} = \omega^{k_{(x,\pm\hat{i})}}$ of the operators V_ℓ on the links $\ell = (x, \pm\hat{i})$ of the vertex x:

$$v_{(x,\hat{1})} v_{(x,\hat{2})} v^*_{(x,-\hat{1})} v^*_{(x,-\hat{2})} = 1, \tag{3.19}$$

or, because of (3.13):

$$\sum_{i=1,2} \left(k_{(x,\hat{i})} - k_{(x,-\hat{i})} \right) = 0 \mod N. \tag{3.20}$$ {eq:gauss_law_elec_eigvals}

Given the fact that the k in (3.12) represent the values of the electric field, one can see that (3.20) can be interpreted as a discretized version of the Gauss law $\nabla \cdot \vec{E} = 0$ in two dimensions, for a pure gauge theory where there are no electric charges.

3.2.3 $\mathbb{Z}_N$ Hamiltonian and the Toric Code

The class of models we consider are described by the Hamiltonian [24, 10, 25]:

$$H_{\mathbb{Z}_N}(\lambda) = -\sum_{\square} U_\square - \lambda \sum_{\ell} V_\ell + \text{h.c.}, \tag{3.21}$$ {eq:hamiltonian_base}

where the first sum is over the plaquettes $\square$ of the lattice while the second sum is over the links ℓ. One can easily see that this Hamiltonian is local and gauge-invariant, hence the dynamics it describes it is fully contained in $\mathcal{H}_{\text{phys}}$. Furthermore, the operator $U_\square$ plays the role of a *magnetic* term, to be more precise it is the magnetic flux inside the plaquette $\square$, while V is the *electric*

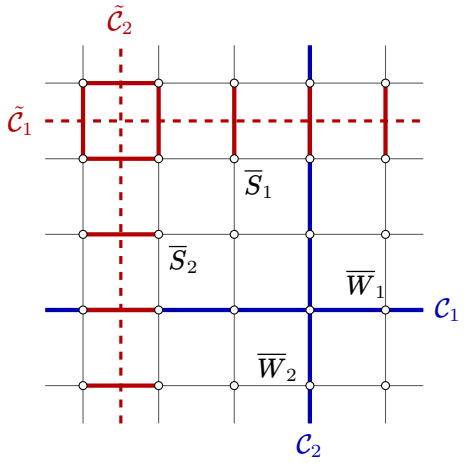

Figure 3.5: Graphical representation of the non-local order parameters $\overline{W}_{1,2}$ (in blue) and $\overline{S}_{1,2}$ (in red) and their respective paths $\mathcal{C}_{1,2}$ and $\tilde{\mathcal{C}}_{1,2}$.

term. The coupling λ tunes the relative strength of the electric and magnetic energy contribution.

These models are akin to the Toric Code [12], which can be thought as a prime example of a $\mathbb{Z}_2$ lattice gauge theory. More precisely, $H_{\mathbb{Z}_2}$ in (3.21) can be thought as a *deformation* of the former, where an external "transverse" field is added to it. Indeed, using the notation used so far, the Toric Code can be formulated as:

$$H_{\mathrm{TC}} = -J_m \sum_{\square} U_{\square} - J_e \sum_{x} G_x. \tag{3.22}$$ {eq:hamiltoniana_toric_code}

whose ground states $|\Psi\rangle$ satisfies the constraints

$$U_{\square}|\Psi\rangle = |\Psi\rangle \quad \forall\, \square, \qquad G_x|\Psi\rangle = |\Psi\rangle \quad \forall x. \tag{3.23}$$ {eq:constraints_gs_toric_cod

Only elementary excitations above the ground state can violate these constraints and they can be of two type: a *magnetic vortex* (which violates the plaquette constraint) or a *electric charge* (which violates the Gauss law). If one imposes $J_e \gg J_m$ to enforce Gauss law, in the low-energy sector there are no electric charges and one recovers the pure gauge $\mathbb{Z}_2$ model of (3.21) for $\lambda = 0$. Therefore, in general the $\mathbb{Z}_N$ models described in (3.21) can be considered as generalization of the Toric Code, from the point of view of lattice gauge theories.

3.2.4 Superselection sectors

Let us consider the Toric Code. One of its main features is the presence of topologically protected degenerate ground states [12]. In order to illustrate

this, besides $\overline{W}_1$ and $\overline{W}_2$, defined in (3.17), another type of non-local operators have to be introduced. They are defined on *cuts* of the lattice $\mathbb{L}$, i.e. paths on the dual lattice $\tilde{\mathbb{L}}$. Consider *non-contractible* cuts $\tilde{\mathcal{C}}_1$ and $\tilde{\mathcal{C}}_2$ along the directions $\hat{1}$ and $\hat{2}$, respectively. On this cuts, the ('t Hooft string) operators $\overline{S}_1$ and $\overline{S}_2$ are constructed as

$$\overline{S}_i = \prod_{\ell \in \tilde{\mathcal{C}}_i} V_\ell, \qquad i = 1, 2, \tag{3.24}$$ {eq:top_string_operators}

in a similar fashion to (3.17). This is shown in red in Fig. 3.5. The operators $\overline{W}_i$ and $\overline{S}_i$ $(i = 1, 2)$ commutes with all the operators $U_\square$ and G_x in the Toric Code Hamiltonian H_{TC} of (3.22), but do not commute with each other. In fact, we have $\overline{W}_i \overline{S}_j = -\overline{S}_j \overline{W}_i$ if $i \neq j$. This means that H_{TC} can be block-diagonalized with respect to the eigenvalues of $\overline{S}_i$ (or $\overline{W}_i$), while $\overline{W}_j$ (or $\overline{S}_j$) connects one block to the other. Furthermore, since in the case of the $\mathbb{Z}_2$ symmetry, $\overline{S}_i$ (or $\overline{W}_i$) has only two eigenvalues (equal to ± 1), there are a total of $2 \times 2 = 4$ degenerates ground states, which are topologically protected, thanks to the fact that $\overline{W}_j$ (or $\overline{S}_j$) cannot be expressed in terms of the local operators $U_\square$ and G_x. Notice that, as it can be easily seen, in the Toric Code the role of $\overline{W}_i$ and $\overline{S}_i$ can be interchanged.

Let us now turn to $\mathbb{Z}_N$ LGT models. The operators $\overline{W}_i$ no longer commute with the Hamiltonian (3.21) which now contains an electric field term. Thus, $\lambda \neq 0$, we have no degenerate ground states. But we can still use the $\overline{S}_i$ operators to decompose the Hilbert space $\mathcal{H}_{\text{phys}}$, since they still commute with all the *local operators* $U_\square$ and V_ℓ (thus also with $H_{\mathbb{Z}_N}$). Now one can see that the operator $\overline{S}_i$ $(i = 1, 2)$ of (3.24) has N eigenvalues ω^n, with $n = 1, \dots, N-1$. Hence, one can decompose $\mathcal{H}_{\text{phys}}$ as sum of superselection sectors

$$\mathcal{H}_{\text{phys}} = \bigoplus_{n,m=0}^{N-1} \mathcal{H}_{\text{phys}}^{(n,m)}, \tag{3.25}$$ {eq:decomposizione_Hphys}

where for each $|\phi\rangle \in \mathcal{H}_{\text{phys}}^{(n,m)}$ we have:

$$\overline{S}_1 |\phi\rangle = \omega^m |\phi\rangle , \quad \overline{S}_2 |\phi\rangle = \omega^n |\phi\rangle . \tag{3.26}$$

Let us consider now the role of the Wilson loops $\overline{W}_i$. One can easily see that:

$$\overline{W}_2 \overline{S}_1 = \omega \overline{S}_1 \overline{W}_2, \qquad \overline{W}_1 \overline{S}_2 = \omega \overline{S}_2 \overline{W}_1. \tag{3.27}$$ {eq:algebra_op_nonlocali}

It follows that $\overline{W}_{1,2}$ acts a shift operators for the eigenspaces of $\overline{S}_{2,1}$:

$$\overline{W}_1 : \mathcal{H}_{\text{phys}}^{(n,m)} \to \mathcal{H}_{\text{phys}}^{(n+1,m)}, \quad \overline{W}_2 : \mathcal{H}_{\text{phys}}^{(n,m)} \to \mathcal{H}_{\text{phys}}^{(n,m+1)}, \tag{3.28}$$ {eq:azione_wilson_loop}

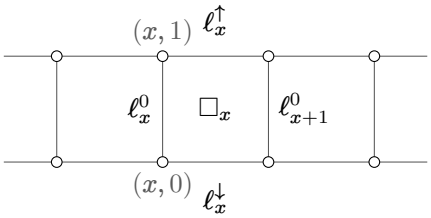

Figure 3.6: Ladder geometry and labeling of its links.

where the integers $n+1$ and $m+1$ have to be taken $\mathrm{mod}\ N$.

From a physical point of view, the Wilson loops operators $\overline{W}_1$ and $\overline{W}_2$ create non-contractible electric loops around the lattice, while the 't Hooft strings $\overline{S}_2$ and $\overline{S}_1$ detect the presence and the strength of these electric loops. Therefore, it is clear that the Hilbert subspace $\mathcal{H}_{\text{phys}}^{(n,m)}$ is the subspace of all the states that contains an electric loop of strength ω^n and ω^m along the $\hat{1}$ and $\hat{2}$ direction, respectively. Furthermore, the evolution of a state in $\mathcal{H}_{\text{phys}}^{(n,m)}$ with the Hamiltonian in (3.21) is confined in $\mathcal{H}_{\text{phys}}^{(n,m)}$.

3.3 Abelian models on the ladder

The main goal of this manuscript is the characterization of the phases of the model described above, but on a ladder geometry. The peculiarity of this geometry is given by the fact that we can study a (quasi)one-dimensional non-trivial LGT with magnetic terms, which are not possible in pure one-dimensional systems. Moreover, since the Hilbert space is highly constrained, we have the possibility to study systems of moderate size through exact diagonalization. The latter will be analyzed in the last section.

A *ladder* is a lattice $\mathbb{L}$ made of two parallels chains, the *legs*, coupled to each other by *rungs* to form square plaquettes. On the ladder, each rung is identified by a coordinate $i = 1, \dots, L$, where L is the length of the ladder, and the two vertices on the rung are denoted with $i^{\uparrow}$ and $i^{\downarrow}$ in the upper and lower leg, respectively. Links are denoted by ℓ. On the legs they are labelled as $\ell_i^{\uparrow}$ (upper leg) or $\ell_i^{\downarrow}$ (lower leg), while on the rungs they are labelled ℓ_i^0.

In order to lighten our notation, we use the symbols V_i^0, U_i^0 for the operators defined on the rung i, and V_i^{ρ}, U_i^{ρ} with $\rho = \uparrow, \downarrow$ for the operators on the horizontal links of the upper and lower leg to the right of the rung. Also, the plaquette operators on the right of the rung i will be labeled as U_i:

$$U_i = U_i^{\downarrow} U_{i+1}^0 (U_i^{\uparrow})^{\dagger} (U_i^0)^{\dagger}. \tag{3.29}$$ {eq:plaq_op_ladder}

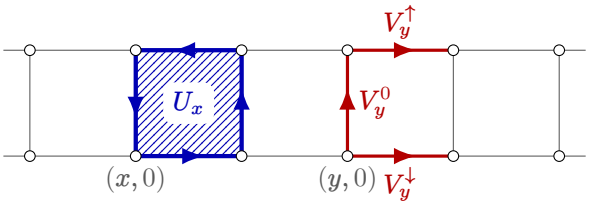

Figure 3.7: Representation of the different ladder operators. On the right: plaquette operator U_x. On the left: the electric operators $V^{\uparrow}$, $V^{\downarrow}$ and V^0.

Moreover, on a ladder only three-legged vertices exist, so the Gauss operators are slightly modified:

$$G_i^{\uparrow} = V_i^{\uparrow}(V_{i-1}^{\uparrow})^{\dagger}(V_i^0)^{\dagger} \text{ and } G_i^{\downarrow} = V_i^{\downarrow}V_i^0(V_{i-1}^{\downarrow})^{\dagger}, \tag{3.30}$$ {eq:gauss_law_ladder}

where $G_i^{\uparrow}$ and $G_i^{\downarrow}$ refers, respectively, to the Gauss operators on the vertices $i^{\uparrow}$ and $i^{\downarrow}$. Finally, we write explicitly the Hamiltonian for a $\mathbb{Z}_N$ LGT on a ladder:

$$H^{\text{lad}}_{\mathbb{Z}_N}(\lambda) = -\sum_i \Big[U_i + \lambda\Big(V_i^{\uparrow} + V_i^{\downarrow} + V_i^0\Big) + \text{h.c.}\Big]. \tag{3.31}$$ {eq:ladder_hamiltonian}

For what concerns topological sectors of the theory, out of the Wilson loop operators in (3.17) only $\overline{W}_1$ is well defined, because we have periodic boundary conditions only along the $\hat{1}$ direction. Hence, only $\overline{S}_2$ in (3.24) (the 't Hooft operator conjugate to W_1) can be used as a mean for distinguishing these different sectors. Therefore the decomposition of the Hamiltonian is realized with blocks of the type $(\omega^k, 1)$, with $k = 0, \dots, N-1$. One of the main features of this decomposition is that, once we have fixed the topological sector, it is possible to write the duality transformation of the block Hamiltonian, which leads to a one-dimensional quantum clock model, with a chiral longitudinal field. The latter is the object of discussion of the following sections.

3.4 Bond-algebraic approach to dualities

Dualities in condensed matter and statistical mechanics have been known for a long time.

One of the most known examples is the self-duality of the Ising model with transverse field [14, 9], which we talked about in [ref della sec sui clock models] This self-duality maps the strong coupling regime into the weak one and vice versa. This mapping make it possible to obtain the critical point, where a quantum phase transition occurs, as the fixed point as its fixed point.

In the following section we will quickly review the bond-algebraic approach to dualities, which is reviewed in [5], because it offers a convenient way for dealing with duality transformations when gauge models are involved. The concept of *bond-algebra* was introduced in [16] and it stems from the fact that most *Hamiltonian are a sum of simple and (quasi)local terms (called bonds)*:

$$H = \sum_{\Gamma} \lambda_{\Gamma} h_{\Gamma}, \tag{3.32}$$

where Γ is a set of indices (e.g. the lattice sites but can be completely general) and λ_{Γ} are numbers. The terms h_{Γ} are the *bond operators* (or simply bonds) and they form a *bond algebra* $\mathcal{A}\{h_{\Gamma}\}$, which is a linear space of operators generated by all the possible powers and products of the bonds h_{Γ} and their Hermitian conjugates.

It is important to point out that a single Hamiltonian H can have different bond algebras associated to it. In fact, a bond algebra is determined by how the bonds of H are decomposed or partitioned. In principle, given any decomposition

$$H = \sum_{\Gamma} \lambda_{\Gamma} h_{\Gamma} = \sum_{\Sigma} \lambda'_{\Sigma} h'_{\Sigma}$$

one should expect $\mathcal{A}\{h_{\Gamma}\} \neq \mathcal{A}\{h'_{\Sigma}\}$ in general (see [5]). Furthermore, the bonds h_{Γ} that generate $\mathcal{A}\{h_{\Gamma}\}$ do not need to be independent.

In this framework, quantum dualities can be formulated as *homomorphisms of bonds algebras*, i.e. structure preserving mappings between bond algebras. To be more precise, two Hamiltonian H_1 and H_2 that act on state spaces of the same dimensions are said to be *dual* if there is some bond algebra $\mathcal{A}_{H_1}$ of H_1 that is homomorphic to some bond algebra $\mathcal{A}_{H_2}$ of H_2 and if the homomorphism $\Phi : \mathcal{A}_{H_1} to \mathcal{A}_{H_2}$ maps H_1 onto H_2, $\Phi(H_1) = H_2$. These mappings do not need to be isomorphisms, especially when gauge symmetries are involved, and we will explain why later.

Dualities, in this approach, are *local* with respect to the bonds, i.e. they map one bond h_{Γ_1} of H_1 to one bond h_{Γ_2} of H_2, which may translates to non-locality with respect to the elementary degrees of freedom. This is due to the fact that the generators of a bond algebra are usually two- (or more) body operators and expressing the elementary degrees of freedom with these operators require large (if not infinite) products.

To make this approach clearer we now apply it to the 1D quantum Ising model with transverse field. The Hamiltonian H_{Ising} of this model

$$H_{\text{Ising}}(\lambda) = \sum_{i} \left(\sigma_i^z \sigma_{i+1}^z + \lambda \sigma_i^x\right) \tag{3.33}$$

where σ_i^x and σ_i^z are the usual Pauli matrices for spin $S = \frac{1}{2}$. We recognize as basic bonds the operators $\{\sigma_i^x\}$ and $\{\sigma_i^z\sigma_{i+1}^z\}$ and their relations can be summarized as follows: (i) each bonds square to the identity operator; (ii) the bonds σ_i^x anticommutes only with $\sigma_i^z\sigma_{i+1}^z$ and $\sigma_{i-1}^z\sigma_i^z$ and commutes with every other bond; (iii) the bonds $\sigma_i^z\sigma_{i+1}^z$ anticommutes only with σ_i^x and σ_{i+1}^x. Given the symmetric roles that the basic bonds σ_i^x and $\sigma_i^z\sigma_{i+1}^z$ play with each other, one can set up a mapping Φ as follows:

$$\Phi(\sigma_i^z\sigma_{i+1}^z) = \sigma_i^x, \qquad \Phi(\sigma_i^x) = \sigma_{i-1}^z\sigma_i^z. \tag{3.34}$$ {eq:duality_ising}

This transformation defined on the bond generators alone extends to the full bond-algebra $\mathcal{A}_{\text{Ising}}$ and it is clear that preserves all the important algebraic relationship and is one-to-one, hence it is an *isomorphism* of $\mathcal{A}_{\text{Ising}}$ onto itself. The Hamiltonian H_{Ising} is just an element of $\mathcal{A}_{\text{Ising}}$ and through Φ gets transformed as

$$\Phi(H_{\text{Ising}}(\lambda)) = \sum_i \left(\sigma_i^x + \lambda\sigma_i^z\sigma_{i+1}^z\right) = \lambda H_{\text{Ising}}(\lambda^{-1}), \tag{3.35}$$

which is just what we stated in [manca eqref] i.e. it maps into itself with inverted couplings.

An isomorphism like Φ is physically sound if it is *unitarily implementable* [5], which means that there is a unitary matrix $\mathcal{U}$ such that the duality isomorphism reads

$$\Phi(\mathcal{O}) = \mathcal{U}\mathcal{O}\mathcal{U}^\dagger, \quad \forall \mathcal{O} \in \mathcal{A}, \tag{3.36}$$

where $\mathcal{A}$ is the operator algebra of the model under investigation.

3.4.1 Gauge-reducing dualities

In this section we will review the notion of *gauge-reducing dualities*. Gauge symmetries are *local symmetries* of the model that signal the presence of *redundant degrees of freedom*, in fact gauge invariance can be thought as a set of *local constraints* on the elementary degrees of freedom of the model. This means that the state space of the model is larger than set of physical states and these are exactly the states that are invariant under the action of the gauge symmetries, which would mean that they satisfies the local constraints of the model. The same can be applied to the Hermitian operators and the observables of the model. An Hermitian operator represent a physical observable only if it commutes with the gauge symmetries, which makes them gauge invariant.

When dealing with a gauge model, it would be natural to assume that, in order to establish a duality with any gauge symmetries, these have to be

eliminated from the former model. In other terms, that it would be necessary to project out the operator content on the subspace of physical states first or proceed with gauge-fixing. Although this is a common and traditional approach to dualities, with bond algebras this is not strictly necessary. As stated in [5], with the bond-algebraic approach one can find mappings to models without any gauge symmetry that preserve all the important algebraic properties.

The procedure goes as follows: consider a gauge model and let H_{G} be its Hamiltonian and G_Γ its gauge symmetries. Naturally, an operator is said to be gauge-invariant only if it commutes with all the G_Γ and clearly the Hamiltonian has to be gauge-invariant, hence $[H, G_\Gamma] = 0$. Now let H_{GR} be the dual Hamiltonian of a non-gauge model. A *gauge-reducing duality* Φ_{GR} maps H_{G} onto H_{GR} while making all the gauge symmetries of the former model trivial, which means:

$$\Phi_{GR}(H_{\mathrm{G}}) = H_{\mathrm{GR}}, \qquad \Phi_{GR}(G_\Gamma) = \mathbb{1}, \quad \forall \Gamma. \tag{3.37}$$

Unlike the dualities in Sec. 3.4, a gauge-reducing duality like Φ_{GR} has to be implementable as a *projective unitary operator* $\mathcal{U}$. Formally, this can be written as

$$\Phi_{\mathrm{GR}}(\mathcal{O}) = \mathcal{U}\mathcal{O}\mathcal{U}^\dagger, \quad \mathcal{U}\mathcal{U}^\dagger = \mathbb{1}, \quad \mathcal{U}^\dagger\mathcal{U} = P_{\mathrm{GI}} \tag{3.38}$$

where P_{GI} is the projector of the subspace of gauge-invariant states, i.e. $G_\Gamma \left|\psi\right\rangle = \left|\psi\right\rangle$ for all Γ. Roughly speaking, this projective unitary operator can be represented as rectangular matrix that preserves the norm of gauge-invariant states while projecting out all the other states.

A clear example of a gauge-reducing duality is provided by the $\mathbb{Z}_N$, $d = 2$ gauge model

$$H_{\mathrm{G}} = \sum_r \left(V_{(r,\hat{1})} + V_{(r,\hat{2})} + \lambda U_r \right). \tag{3.39}$$

Its group of gauge symmetries is generated by (3.14). In the simplest case where $N = 2$, the V's can be represented by the Pauli operators σ^z and the U's by σ^x. In so doing, the Gauss operator becomes

$$G_r = \sigma^z_{(r,\hat{1})}\sigma^z_{(r,\hat{2})}\sigma^z_{(r,-\hat{1})}\sigma^z_{(r,-\hat{2})}, \tag{3.40}$$ {eq:gauss_operator_Z2}

and commutes with H_{G} and with the bonds $\left\{\sigma^z_{(r,\hat{1})},\ \sigma^z_{(r,\hat{2})},\ U_r\right\}$. In other words, the bond algebra they generate is gauge-invariant, and satisfy three simple relations: (i) all the bonds square to the identity, (ii) each spin σ^z anti-commutes with two adjacent plaquettes operators U, and (iii) each plaquette operator U anti-commutes with four spins σ^z. This set of relations are identical

to those satisfied by the bonds of the $d = 2$ quantum Ising model, and the mapping is the following:

$$\begin{aligned} \Phi\left(\sigma^z_{(r,\hat{1})}\right) &= \sigma^x_{(r-\hat{2})}\sigma^x_r, \\ \Phi\left(\sigma^z_{(r,\hat{2})}\right) &= \sigma^x_{(r-\hat{1})}\sigma^x_r, \\ \Phi(U_r) &= \sigma^z_r. \end{aligned} \tag{3.41}$$ {eq:duality_2d}

Thus, Φ maps H_{G} to H_{Ising}, if we identify the constants $\lambda \leftrightarrow h$ and $1 \leftrightarrow J$. Moreover, Φ is a gauge-reducing duality homomorphism, since $\Phi(G_r) = \mathbb{1}$. Therefore, H_{Ising} represents all the physics contained in H_{gauge}, but without all the gauge redundancies. In the general case, i.e. for a generic $\mathbb{Z}_N$ symmetry, the duality leads to an N-clock model [20].

3.5 Dualities in two dimensions

[da scrivere]

3.6 Dualities of the ladder

3.6.1 Clock models

In this section we will deal with a class of generalizations of the quantum Ising model known as *clock models* [7, 2], which shows a resemblance to the $\mathbb{Z}_N$ LGT models we introduced previously. This similarity will later be exploited in order to obtain a complete description of the LGT models without any redundant gauge-symmetry.

For a discussion about clock models we start from the Hamiltonian of the quantum Ising model with a transverse field, which can simply be written as

$$H = -\sum_i \sigma^z_i \sigma^z_{i+1} - h\sum_i \sigma^x_i, \tag{3.42}$$ {eq:ising_hamiltonian_duality

where $\sigma^{x,z}_i$ are the usual 2×2 Pauli matrices for each site i:

$$\sigma^x_i = \begin{pmatrix} 0 & 1 \\ 1 & 0 \end{pmatrix}, \quad \sigma^z_i = \begin{pmatrix} 1 & 0 \\ 0 & -1 \end{pmatrix}. \tag{3.43}$$

They are a set of unitary matrices that commute on different sites, while on the same site they anticommute $\sigma^x\sigma^z = -\sigma^z\sigma^x$. Another way to put it is to say that the exchange of σ_x and σ_z on the same site produces a phase $e^{i\pi} = -1$.

Clock models can be thought as generalizations of the quantum Ising model, but not to higher spins. A p-state clock model (or simply a p-clock model) utilizes a set of unitary operators that generalize the algebra of Pauli matrices in the following sense: the operators σ_x and σ_z get promoted to the *clock operators* X and Z, respectively, which are $p \times p$ unitary matrices whose exchange produces a phase $\omega = e^{i2\pi/p}$, instead of -1. The algebraic properties of these clock operators X and Z can be summarized as follows:

$$\begin{aligned} XZ &= \omega ZX, & X^p &= Z^p = \mathbb{1}_p, \\ X^\dagger &= X^{-1} = X^{p-1}, & Z^\dagger &= Z^{-1} = Z^{p-1} \end{aligned} \tag{3.44}$$ {eq:clock_operator_algebra}

We see that the Schwinger-Weyl algebra in (3.12) and the clock operator algebra in (3.44) are basically the same, but there are some key differences to point out betweens a $\mathbb{Z}_N$ LGT and a p-clock model.

The degrees of freedom of a $\mathbb{Z}_N$ LGT live on the links of the lattice while in a p-clock model they live on the sites. But the most important aspect is that we don't have any gauge symmetry in a p-clock model, hence we do not have to impose any local constraints or physical conditions. These models can be derived as the quantum Hamiltonians of the classical 2D vector Potts model, which is a discretization of the 2D planar XY model [18].

A typical p-clock model Hamiltonian with transverse field has the form

$$H_{\text{clock}}(\lambda) = -\sum_i Z_i Z_{i+1} - \lambda \sum_i X_i + \text{h.c.} \tag{3.45}$$ {eq:clock_hamiltonian}

which is, as expected, very similar to the quantum Ising Hamiltonian in (3.42). Furthermore, just like the latter, p-clock models with only transverse field are *self-dual*: the clocks can be mapped into the kinks (or domain walls) and one would obtain the same exact Hamiltonian description but with inverted transverse field [18]. For $p < 5$, the clock models presents a self dual point in $\lambda = 1$, that separates an ordered phase from a disordered one. On the other hand, for $p \geq 5$ we have an intermediate continuous critical phase between the ordered and disordered phase with two BKT transition points, which are related to each other through the self-duality [23].

These models have been thoroughly studied, even with the addition of a longitudinal field $\propto Z_i$ [3] or chiral interactions. In particular, in the case of chiral interactions, it was shown [8] that the Hamiltonian (3.45) can be mapped to a parafermionic chain through a Fradkin-Kadanoff transformation, and in presence of a $\mathbb{Z}_3$ symmetry, it shows three different phases [29], if open boundaries are implemented: a trivial, a topological and an incommensurate (IC) phase. The case which presents a real longitudinal field term was considered in [11], where some of the critical exponents have been estimated.

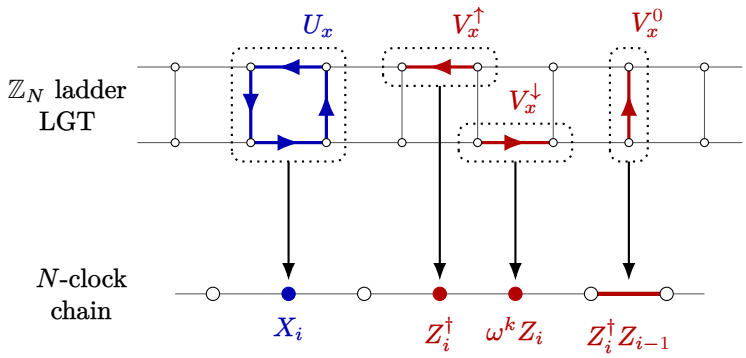

Figure 3.8: Visual representation of the duality transformation from the $\mathbb{Z}_N$ ladder LGT to the N-clock model. The plaquette operator U_x and the electric operators $V^{\uparrow}$ and $V^{\downarrow}$ map to one-site operators in the clock model, while the remaining electric operator V^0 maps to a hopping term between nearest neighbouring sites.

The general case, where chiral interactions are included in a $\mathbb{Z}_N$ model, has been studied in [8]. Here, the author considered the model as an extension of the Ising/Majorana chain and found the edge modes of the theory. He also calculated the points, in the parameter space, where the model is integrable or 'superintegrable'. All these studies are motivated by theoretical interest and recent experiments, which can be analysed by the above models [4].

3.6.2 Duality onto clock models

In this section we will show how to construct a mapping of the $\mathbb{Z}_N$ ladder LGT onto a N-clock model on a chain with a transversal field and a longitudinal field, the latter depending on the topological sector of the ladder LGT.

The first step is the decomposition of the set of bonds in (3.21). Obviously, the magnetic terms $U_{\square}$ have to be separated from the electric terms V_ℓ, but the latter cannot be all treated the same. It is clear from the geometry of the ladder, that the links ℓ^0 have a different role when compared with the links $\ell^{\uparrow}$ and $\ell^{\downarrow}$, because the former are *domain walls* while the latter are not. Therefore, the duality transformation has to distinguish between the vertical links and horizontal links. Furthermore, also the top links $\ell^{\uparrow}$ and bottom links $\ell^{\downarrow}$ have to be treated separately because the electric operator on them have different commutation relations with the plaquette operators. In fact, using the notation introduced in Sec. 3.3, we have

$$U_x V_x^{\downarrow} = \omega V_x^{\downarrow} U_x, \qquad U_x V_x^{\uparrow} = \omega^{-1} V_x^{\uparrow} U_x. \tag{3.46}$$ {eq:comm_rel_ladder}

and indeed they acquire different phases.

The plan is to associate to each plaquette a clock degree of freedom, hence we identify a plaquette $\square_x$ with a site i of a clock chain and the magnetic flux of a plaquette becomes the "fundamental gauge invariant degree of freedom" of the LGT ladder model. Given the fact that we are working in the electric basis, we chose for convenience to map the $\mathbb{Z}_N$ magnetic operator U_x to the "momentum" operator X_i of the N-clock chain. The electric field on a vertical link ℓ^0 is the result of the flux difference between the two plaquettes that it separates, which suggests that the operator V_{ℓ^0} have to be mapped to a kinetic-type term like $Z_i^\dagger Z_{i-1}$. This can be readily verified. From (3.29) we get

$$V_x^0 U_x = \omega^{-1} U_x V_x^0, \qquad V_x^0 U_{x-1} = \omega U_{x-1} V_x^0,$$

therefore the maps

$$U_x \mapsto X_i, \qquad V_x^0 \mapsto Z_i^\dagger Z_{i-1},$$

clearly conserves the commutation relations of U_x and V_x^0.

For now we are left with task of finding a suitable mapping of $V^\uparrow$ and $V^\downarrow$. With respect to the other bonds of the theory, both of them commute with V^0 while for (3.46) holds for U_x. Hence, a suitable and general mapping of $V^\uparrow$ and $V^\downarrow$ can be:

$$V_x^\downarrow \mapsto c_i^\downarrow Z_i, \qquad V_x^\uparrow \mapsto c_i^\uparrow Z_i^\dagger, \tag{3.47}$$

{eq:elec_op_horiz_ladder_ma

where $c_i^\downarrow$ and $c_i^\uparrow$ are complex numbers. Although, they cannot be any complex number. Both $V_x^\downarrow$ and $V_x^\uparrow$ have to be mapped onto unitary operators, which limits the numbers $c_i^\downarrow$ and $c_i^\uparrow$ to be *complex phases*.

To further constraint the value of these coefficients, we can use the Gauss law. In particular, given the fact that we are looking for a gauge-reducing duality, the aim is to make the Gauss law trivial. Using the mappings (3.6.2) and (3.47) in (3.30) yields

$$\begin{aligned} G_x^\uparrow &\mapsto (c_i^\uparrow Z_i^\dagger)(c_{i-1}^\uparrow Z_{i-1}^\dagger)(Z_i^\dagger Z_{i-1})^\dagger = c_i^\uparrow (c_{i-1}^\uparrow)^*, \\ G_x^\downarrow &\mapsto (c_i^\downarrow Z_i^\dagger)(Z_i^\dagger Z_{i-1})(c_{i-1}^\downarrow Z_{i-1}^\dagger) = c_i^\downarrow (c_{i-1}^\downarrow)^* \end{aligned} \tag{3.48}$$

{eq:gauss_law_map_ladder}

Gauss law have to be satisfied in a pure gauge theory, which mean that we have to impose $G_x^\uparrow = \mathbb{1}$ and $G_x^\downarrow = \mathbb{1}$ for all x. This is only possible if

$$c_i^\downarrow = c^\downarrow, \qquad c_i^\uparrow = c^\uparrow, \qquad \forall i. \tag{3.49}$$

Furthermore, thanks to (3.48) we also know how to introduce static matter into this duality, because it can be thought as a violation of the Gauss law. We just have to change the phases $c_i^\uparrow$ and $c_i^\downarrow$.

The last factor to consider is how the $c^\uparrow$ and $c^\downarrow$ are related on the same site i. In this regard, the topological sectors of the theory come to the rescue. As

established in Sec. 3.3, the topological sectors are identified by the eigenvalue of S_2 in (3.24), which in the ladder geometry becomes

$$S_2 = V_x^{\uparrow} V_x^{\downarrow} \tag{3.50}$$ {eq:top_string_op_ladder}

for any fixed x. Its eigenvalue are simply ω^k, for $k = 0, \dots, N-1$.

Given a topological sector ω^k, using the mapping (3.47) on (3.50) yields

$$S_2 \;\longmapsto\; (c^{\uparrow} Z_i^{\dagger})(c^{\downarrow} Z_i) = c^{\uparrow} c^{\downarrow} = \omega^k. \tag{3.51}$$

From here, in order to solve for the coefficients $c^{\uparrow}$ and $c^{\downarrow}$, one needs only to fix one of the to 1 and the other to ω^k. We choose to fix these coefficients as follows:

$$c^{\uparrow} = 1, \qquad c^{\downarrow} = \omega^k. \tag{3.52}$$

In conclusion, we summarize the duality mapping for the topological sector ω^k of the $\mathbb{Z}_N$ LGT on a ladder:

$$\begin{aligned} U_x &\longmapsto X_i, \qquad & V_x^0 &\longmapsto Z_i^{\dagger} Z_{i-1}, \\ V_x^{\uparrow} &\longmapsto Z_i^{\dagger}, \qquad & V_x^{\downarrow} &\longmapsto \omega^k Z_i. \end{aligned} \tag{3.53}$$ {eq:ladder_duality}

With the duality (3.53), from (3.31) in the sector $(\omega^k, 1)$ we obtain

$$H_{\text{ladder}}(\lambda) \;\longmapsto\; \lambda H_{\text{clock}}(\lambda^{-1}) \tag{3.54}$$

where

$$H_{\text{clock}}(\lambda^{-1}) = -\sum_i Z_i^{\dagger} Z_{i-1} - \lambda^{-1} \sum_i X_i - (1+\omega^k) \sum_i Z_i + \text{h.c.} \tag{3.55}$$ {eq:dual_ladder_hamiltonian}

We see that (3.55) is a clock model with both *transversal* and *longitudinal* fields. In particular, the longitudinal field carries the information of the topological sector of the ladder model.

Interestingly, for N even the sector $k = N/2$ has a special role. Within this sector $\omega^k = -1$, for which the *longitudinal field disappears* and H_{clock} reduces to self-dual quantum clock models with a known quantum phase transition. This phase transitions for $k = N/2$ can be put in correspondence with a *confined-deconfined* transition, which will be discussed in much more detail in the next section.

Let us remark that the complex coupling $(1+\omega^n)$ does not make the Hamiltonian (3.55) necessarily chiral [8, 27]. In fact, one can get the real Hamiltonian

$$H_N = H_p(1/\lambda) - 2\cos\left(\frac{\pi n}{N}\right) \sum_i \left(Z_i + Z_i^{\dagger}\right). \tag{3.56}$$ {eq:dual_ladder_hamiltonian}

by absorbing the complex phase in the Z_i-operators, with the transformation $Z_i \mapsto w^{-n/2} Z_i$. This transformation globally rotates the eigenvalues of the Z_i-operators, while preserving the algebra relations. For n even, this is just a permutation of the eigenvalues, meaning that it does not affect the Hamiltonian spectrum. Instead, for n odd, up to a reorder, the eigenvalues are shifted by an angle π/N, i.e. half the phase of ω. The energy contribution of the extra term in (3.56) depends on the real part of these eigenvalues and for n odd we obtain that the lowest energy state is no longer unique, in fact it is doubly degenerate. This means that for $\lambda \to \infty$, where the extra term becomes dominant, we expect an ordered phase with a doubly degenerate ground state. Finally, one can easily prove that the sectors n and $N - n$ are equivalent [1].

3.7 A case study: $N = 2, 3$ and 4

3.7.1 Investigating the phase diagram

We wish to study the phase diagram of the $\mathbb{Z}_N$ LGT phase diagram, in particular we are interested in any *confined* or *deconfined* phase. In a pure gauge theory, these phases are investigated non-local order parameters like the *Wilson loop* (not be confused with the non-contractible Wilson loops in (3.17)) or *string tension*. This is because we expect the deconfined phase to be a topological phase, which can be investigated only with non-local order parameters.

Given a closed region $\mathcal{R}$, a Wilson loop operator $W_{\mathcal{R}}$ is defined as

$$W_{\mathcal{R}} = \prod_{\square \in \mathcal{R}} U_{\square}. \tag{3.57}$$ {eq:closed_wilson_loop}

Alternatively, considering the oriented boundary $\partial\mathcal{R}$ one can write

$$W_{\mathcal{R}} = \prod_{\ell \in \partial\mathcal{R}} U_{\ell}, \tag{3.58}$$

where the Hermitian conjugate is implied everytime we move in the negative directions. It is also implied that the curve $\partial\mathcal{R}$ is a contractible loop. Wilson showed in [28] that quark confinement is related to the expectation value $\langle W_{\mathcal{R}} \rangle$ of a Wilson loop, which can be thought as a gauge field average on a region. In particular, in the presence of quark confinement the gauge field average follows an *area law*, where it decays exponentially with the area enclosed by $\mathcal{R}$. On the other hand, in the deconfined phase we have a *perimeter law*, where the gauge field average decays exponentially with the perimeter of $\mathcal{R}$.

[1] For the sector $N - n$ we have that the overall factor $\cos(\pi(N-n)/N)$ is just $-\cos(\pi n/N)$. The minus sign can then be again absorbed into the Z's operators. This overall operation is equivalent to the mapping $Z \mapsto \omega^{-n/2} Z$ for the sector $N - n$.

Unfortunately on a ladder geometry there is not much difference between the area and the perimeter of a Wilson loop. In fact, in units of the lattice spacing, the area of a Wilson loop over n plaquettes is n while its perimeter is just $2n + 2$. They both grow linearly. Nonetheless, we can still look at the behaviour of the Wilson loop, for a fixed length, at different couplings λ.

When the coupling λ in (3.21) is equal to zero, the Toric Code is recovered and in any of its topological sector the ground state is the equal superposition of all the states with any number of closed electrical loops, in a similar fashion to coherent states. This makes the Toric Code a *quantum loop gas*, which is a *deconfined phase*. Furthermore, the operator $W_{\mathcal{R}}$ in (3.57) creates an electrical loop around the region $\mathcal{R}$. From the constraints (3.23), it can easily be proved that $W_{\mathcal{R}}$ leaves the Toric Code ground states unchanged, showing in fact that they behaves as coherent states, which leads to $\langle W_{\mathcal{R}} \rangle = 1$.

Therefore, $\langle W_{\mathcal{R}} \rangle \approx 1$ signals a deconfined phase and on the other hand a vanishing $\langle W_{\mathcal{R}} \rangle \approx 0$ corresponds to confined phase. For this reason, even tough we lack an area/perimeter law on the ladder geometry it is still sensible to look at the behaviour of the Wilson loop.

Another possible approach for investigating the phase diagram is to use the *string tension*. In two dimensions, given an *open* curve $\tilde{\mathcal{C}}$ on the dual lattice $\tilde{\mathbb{L}}$ we can construct an open 't Hooft string operator $S_{\tilde{\mathcal{C}}}$ as

$$S_{\tilde{\mathcal{C}}} = \prod_{\ell \in \tilde{\mathcal{C}}} V_\ell \tag{3.59}$$

with the usual caveat: we have to take the Hermitian conjugate everytime the path goes in the negative direction. Then the string tension is just the expectation value $\langle S_{\tilde{\mathcal{C}}} \rangle$ it is called in this way because it related to the potential energy (tension) between two magnetic fluxes created at the ends of the curve $\tilde{\mathcal{C}}$. Henceforth, in a deconfined phase $\langle S_{\tilde{\mathcal{C}}} \rangle \approx 0$, which means that the magnetic fluxes can be moved freely with no cost in energy, like in the Toric Code.

3.7.2 Implementing the Gauss law

In order to proceed with ED one has to provide two things: (i) the basic operators of the theory (U_ℓ and V) and (ii) the physical (gauge-invariant) Hilbert space, given a lattice with specified size and boundary conditions. The former was fairly standard while the latter was the most challenging and interesting part to implement.

If one has to work with only physical states, then one has to check the Gauss law for every site. With the brute-force method one has to generate all the possible states and then filter out all the states that violate Gauss law. This method, like any brute-force method, is not very efficient. To better

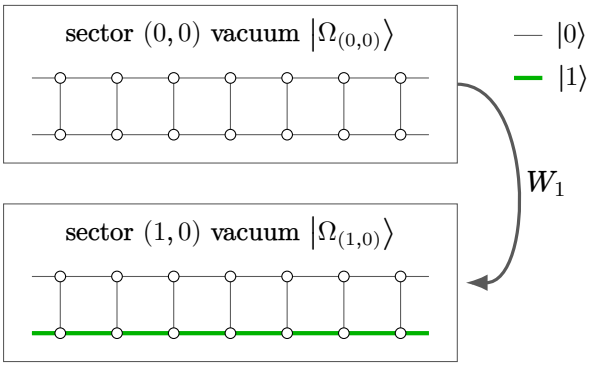

Figure 3.9: The different "Fock vacua" $\left|\Omega_{(0,0)}\right\rangle$ and $\left|\Omega_{(1,0)}\right\rangle$ of the $\mathbb{Z}_2$ ladder LGT. The latter can be obtained from the former by applying the Wilson loop operator W_1. The states $|0\rangle$ and $|1\rangle$ refers to the eigenstates of the electric field operator V, which is just σ_z in the $\mathbb{Z}_2$ model.

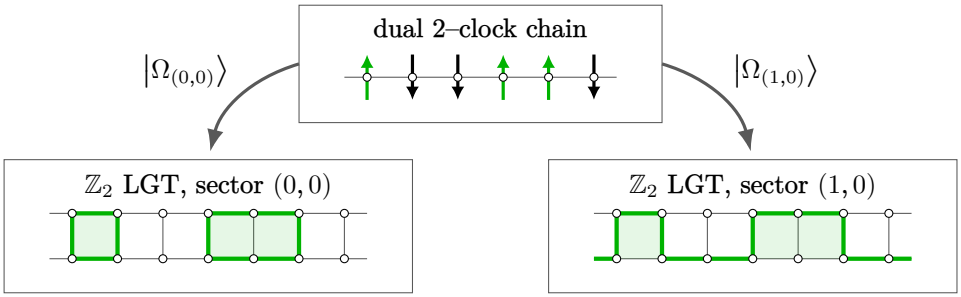

Figure 3.10: Duality between the states of a 2–chain and the states of a $\mathbb{Z}_2$ ladder LGT in the different sectors $(0,0)$ (no non-contractible electric loop) and $(1,0)$ (one non-contractible loop around the ladder). In the sector $(0,0)$ it is evident that all the physical states contains closed electric loops. On the other hand, in the sector $(1,0)$ the physical states are all the possible deformation of the electric string that goes around the ladder.

exemplify this, consider a $\mathbb{Z}_2$ theory on a $L \times L$ periodic lattice, which have L^2 sites and $2L^2$ links. There are therefore 2^{2L^2} possible states and for each one up to L^2 checks (one per site) has to be performed. Moreover, it can be showed that there are only 2^{L^2} *physical* states. As a result, the construction of the physical Hilbert space involves $O(L^2 2^{2L^2})$ operations in a search space of 2^{2L^2} objects for finding only 2^{L^2} elements. All of this makes the inefficiency of this brute-force method very clear, even for moderately small lattices.

The approach adopted in this work exploits the duality in Sec. 3.6 and represents an *exponential speedup* with respect to the brute-force method. It is not a search or pattern-matching algorithm, each physical configuration is

procedurally generated from the states of the dual clock model.

Given a $\mathbb{Z}_N$ LGT on a lattice of size $L \times L$, we consider the dual N-clock model on a similar lattice with $A = L^2$ sites, In its Hilbert space $\mathcal{H}_{N\text{-clock}}$ there is no gauge constraint or physical condition to apply, hence the basis is the set of states $|\{s_i\}\rangle \equiv |s_0 s_1 \cdots s_{A-1}\rangle$ with each $s_i = 0, \ldots, N-1$. From a state $|\{s_i\}\rangle$ we can obtain the dual state for the LGT model in the (m, n) sector:

$$|\{s_i\}\rangle \longmapsto \prod_{i=0}^{A-1} U_i^{s_i} \left|\Omega_{(n,m)}\right\rangle, \tag{3.60}$$

where U_i is the plaquette operator on the i-th plaquette and $\left|\Omega_{(m,n)}\right\rangle$ is the "Fock vacuum" of the (m, n) sector. As one can deduce, the information about the topological sector of the LGT model is carried in the Hamiltonian $H_{N\text{-clock}}$ of the dual clock model and not in the structure of $\mathcal{H}_{N\text{-clock}}$. This means that is possible to build each sector $\mathcal{H}_{\text{phys}}^{(n,m)}$ in (3.25) from $\mathcal{H}_{N\text{-clock}}$, with the appropriate $\left|\Omega_{(n,m)}\right\rangle$.

Moreover, also the "Fock vacuums" $\left|\Omega_{(n,m)}\right\rangle$ can be obtained easily, thanks to (3.28):

$$\left|\Omega_{(n,m)}\right\rangle = (W_1)^n (W_2)^m \left|\Omega_{(0,0)}\right\rangle, \tag{3.61}$$

where $\left|\Omega_{(0,0)}\right\rangle$ is just the state $|000\cdots0\rangle$ (in the electric basis) for all the links.

If we want to quantify the obtained speedup with this method, in the case of a $\mathbb{Z}_2$ theory on a square lattice $L \times L$ there are 2^{L^2} possible clock configurations. For each configuration, there are at most L^2 magnetic fluxes to apply. This translates into $O(L^2 2^{L^2})$ operations, which is an exponential speedup with respect to the brute-force (notice the lack of a factor 2 in the exponent) and is easily generalizable for any $\mathbb{Z}_N$. Although, it remains an open question whether a similar method can be applied for gauge theories with non-Abelian finite groups.

3.7.3 Non-local order parameters

In Sec. 3.7.1 we talked about how a Wilson loop $W_{\mathcal{R}}$ or an 't Hooft string $S_{\tilde{\mathcal{C}}}$ work as a non-local order parameters and can be used to investigated the phase diagram of a $\mathbb{Z}_N$ LGT model. In fact, we analyzed these exact observables on the ladder geometry for $N = 2, 3$ and 4. Given a ladder of length L, the Wilson loop W have been calculated over a region that covers the first $L/2$ plaquettes, while the 't Hooft string cuts through the first $L/2$ plaquettes (see Fig. 3.11).

We wish to investigate the presence of a *deconfined-confined phase transition* (DCPT) for a given $\mathbb{Z}_N$ ladder LGT. In a pure gauge theory, these phases

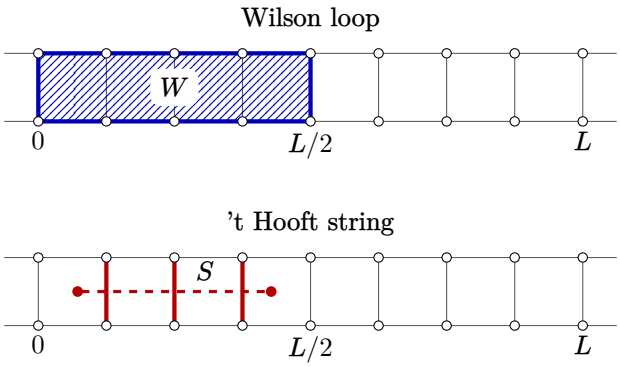

Figure 3.11: The non-local order parameters that have been used for investigating the phase diagram of $\mathbb{Z}_N$ ladder LGT. *Top*: half-ladder Wilson loop. *Bottom*: half-ladder 't Hooft string operator.

can be detected with the perimeter/area law for Wilson loops [28], which can be expressed as the products of magnetic operators over a given region. Unfortunately, in a ladder geometry there is not much difference between the area and the perimeter of a loop, since they both grow linearly in the size system L.

Nonetheless, we expect a phase transition by varying λ [25, 10, 24] that can still be captured by an operator like $W_{\mathcal{R}} = \prod_{i\in\mathcal{R}} U_i$, the product of magnetic operators U's over a (connected) region $\mathcal{R}$. Indeed, when $\lambda = 0$, the Hamiltonian (3.31) is analogous to a Toric Code [12] which is known to be in a deconfined phase, where the (topologically distinct) ground states are obtained as uniform superpositions of the gauge-invariant states, i.e. closed electric loops. On these ground states $\langle W_{\mathcal{R}}\rangle = 1$, hence a value $\langle W_{\mathcal{R}}\rangle \approx 1$ signals a deconfined phase. On the other hand, when $\lambda \to \infty$, the electric loops are suppressed, hence $\langle W_{\mathcal{R}}\rangle \approx 0$, signalling a confined phase.

In the dual clock model picture, the Wilson loop translates to a disorder operator [9], which means that a deconfined phase can be thought of as a paramagnetic (or disordered) phase, while the confined phase is like a ferromagnetic (or ordered) phase. Moreover, the longitudinal field breaks the N-fold symmetry of the ferromagnetic phase into a one-fold or two-fold degeneracy, depending on the parity (n even/odd) of the superselection sector.

We study the $\mathbb{Z}_N$ LGT on a ladder numerically through *exact diagonalization*, by evaluating the half-ladder Wilson loop, i.e.

$$W = U_1 U_2 \cdots U_{L/2}, \tag{3.62}$$

and working in the restricted physical Hilbert space $\mathcal{H}^{(n)}_{\text{phys}}$ ($n = 0, \ldots, N-1$),

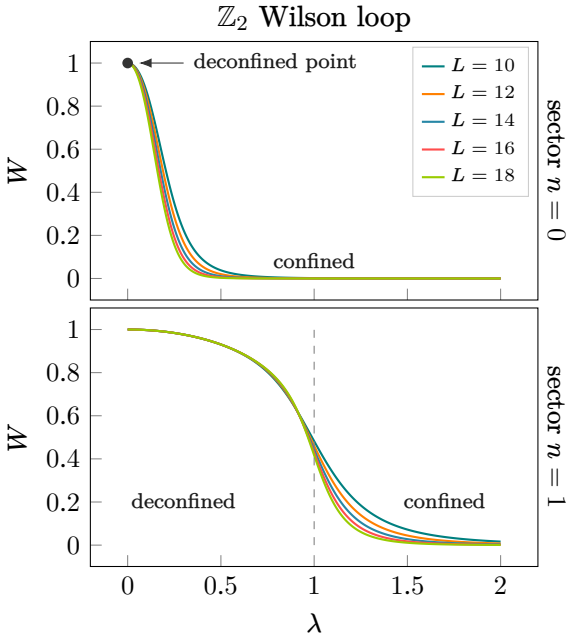

Figure 3.12: $\mathbb{Z}_2$ Wilson loop in the sectors $n = 0$ (*top*) and $n = 1$ (*bottom*), for sizes $L = 10, 12, \ldots, 18$. The sector $n = 0$ presents only a deconfined point at $\lambda = 0$ and then decays rapidly into a confined phase, while the sector $n = 1$ has a phase transition for $\lambda \simeq 1$.

which has dimension N^L, much smaller than N^{3L} (the dimension of the total Hilbert space).

The naive and brute-force method for building $\mathcal{H}_{\text{phys}}$ would require checking the Gauss law at every site (which are $O(3L)$ operations) for all the possible N^{3L} candidate states. On the other hand, the gauge-reducing duality to clock models provides a faithful and efficient method for building the N^{L+1} basis states of $\mathcal{H}_{\text{phys}}$, yielding a major speedup with respect to the naive method. The procedure is quite simple and it consists in treating a clock state as a plaquette flux state in the following way. Let $|\Omega_0\rangle$ be the vacuum state where all the links are in the $|0\rangle$ state. For each sector n we can build a "vacuum" state $|\Omega_n\rangle$ by applying $\overline{W}$ in (3.17) n times on the true vacuum, i.e. $|\Omega_n\rangle = \overline{W}^n |\Omega_0\rangle$. Then, let $|s_1 s_2 \cdots\rangle$ be a configuration of the dual N-clock model, where $s_i = 0, \ldots, N-1$. Now, the equivalent ladder state in the n-th sector can be obtained with $\prod_i U_i^{s_i} |\Omega_n\rangle$.

In the following, we present the results with $N = 2, 3$ and 4, for different lengths.

Results for $N = 2$ As a warm up, we consider the $\mathbb{Z}_2$ ladder LGT, with lengths $L = 10, 12, \ldots, 18$. This model is equivalent to a $p = 2$ clock model, which is just the quantum Ising chain, with only two superselection sectors for $n = 0$ and $n = 1$. When $n = 1$, the Hamiltonian contains only the transverse filed and is integrable [3]. Thus, we expect a critical point for $\lambda \simeq 1$, which will be a DCPT in the gauge model language. This is clearly seen in the behaviour of the half-ladder Wilson loop, as shown in the lower panel of Fig. 3.12. For $n = 0$, both the transverse and longitudinal fields are present, the model is no longer integrable [1, 13, 19] and we expect to always see a confined phase, except for $\lambda = 0$. This is indeed confirmed by the behaviour of the half-ladder Wilson loop shown in the upper panel of Fig. 3.12.

We can further characterize the phases of the two sectors by looking at the structure of the ground state, for $\lambda < 1$ and $\lambda > 1$, which is possible thanks to the exact diagonalization. In particular, in the deconfined phase of the sector $n = 1$, the ground state is a superposition of the deformations of the non-contractible electric string that makes the $n = 1$ vacuum $|\Omega_1\rangle$. For this reason, this phase can be thought as a *kink condensate* [9] (which is equivalent to a paramagnetic phase), where each kink corresponds to a deformation of the string. Instead, for $\lambda > 1$, where we have confinement (as in the $n = 0$ sector), the ground state is essentially a product state, akin to a ferromagnetic state.

Results for $N = 3$ The $\mathbb{Z}_3$ LGT is studied for lengths $L = 7, 9, 11$ and 13. This model can be mapped to a 3-clock model, which is equivalent to a 3-state quantum Potts model with a longitudinal field, which is present in all sectors, as one can see from (3.56). This field is expected to disrupt any ordered state and thus it is not possible to observe a phase transition, as it is confirmed by the behaviour of the half-ladder Wilson loops shown in Fig. 3.13. In addition, all the sectors present a deconfined point at $\lambda = 0$. In the case $n = 0$, for $\lambda > 0$ we recognize a quick transition to a confined phase, similar to what happens in [17]. While for $n = 1$ and 2 (which are equivalent), the model exhibits a smoother *crossover* to an ordered phase characterized by a doubly-degenerate ground state, for $\lambda > 1$. Notice that, as discussed above, the presence of the "skew" longitudinal field breaks the three-fold degeneracy expected in the ordered phase of the 3-clock model into a two-fold degeneracy only.

Results for $N = 4$ The $\mathbb{Z}_4$ ladder LGT have four superselection sectors. The behaviour of half-ladder Wilson loops as function of λ is shown in Fig. 3.14. As in the previous models, for $n = 0$ we see a deconfined point at $\lambda = 0$, followed by a sharp transition to a confined phase. The sector $n = 2$, which

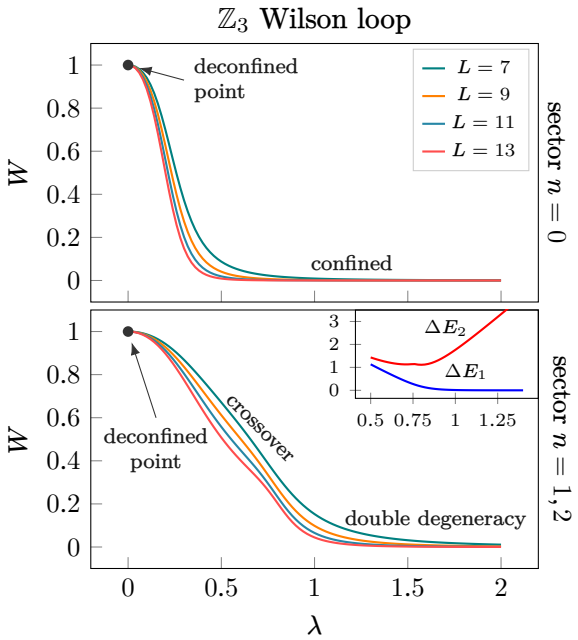

Figure 3.13: $\mathbb{Z}_3$ Wilson loop for the sectors $n = 0$ (*top*) and $n = 1, 2$ (*bottom*, which are equivalent), for sizes $L = 7, 9, 11$ and 13. Inset: energy differences $\Delta E_i = E_i - E_0$ for $i = 1, 2$, as a function of the coupling λ, in the sectors $n = 1, 2$, showing the emergence of a double-degenerate ground state for $\lambda > 1$.

has no longitudinal field, is the only one to present a clear DCPT for $\lambda \approx 1$, as it is expected from the fact that the 4-clock model is equivalent to two decoupled Ising chains [18]. In the two equivalent sectors $n = 1$ and 3, where the longitudinal field is complex, the Wilson loop shows a peculiar behaviour, at least for the largest size ($L = 10$) of the chain: it decreases fast as soon $\lambda > 0$, to stabilize to a finite value in the region $0.5 \lesssim \lambda \lesssim 1$, before tending to zero. The characteristics of this phase would deserve a deeper analysis, that we plan to do in a future work. For $\lambda \gtrsim 1$, the system enters a deconfined phase with a double degenerate ground state, as for the $\mathbb{Z}_3$ model.

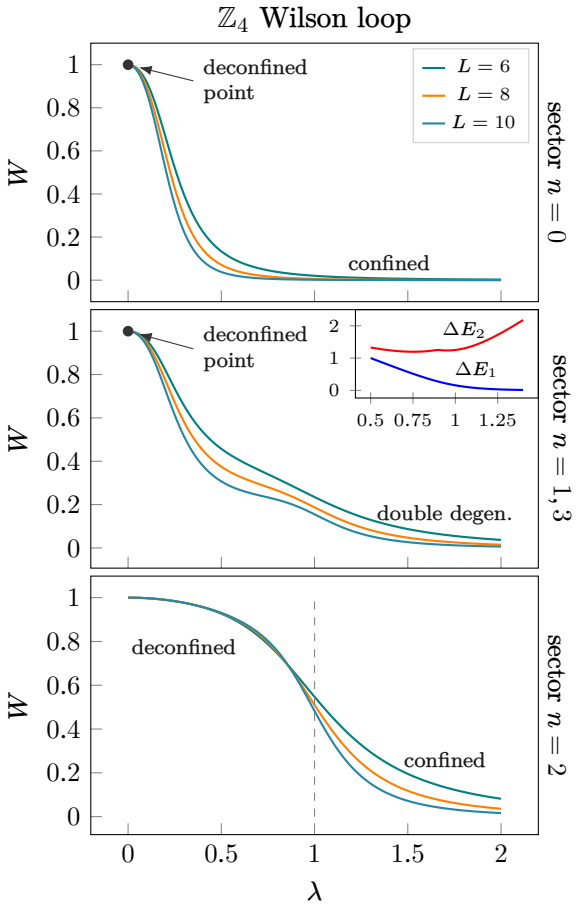

Figure 3.14: $\mathbb{Z}_4$ Wilson loop for sectors $n = 0, \ldots, 3$ and sizes $L = 6, \ldots, 10$. Only the sector $n = 2$ has a clear deconfined-confined phase transition, as expected from the duality with the 4-clock model.